

TRANSCRIPTIONAL AND EPIGENETIC REGULATORY PROGRAMS IN
HEMATOPOIESIS AND LEUKEMOGENESIS

by
Jessica Gucwa

A dissertation submitted to Johns Hopkins University in conformity with the
requirements for the degree of Doctor of Philosophy

Baltimore, Maryland
November, 2016

© 2016 Jessica Gucwa
All Rights Reserved

ABSTRACT

The hematopoietic system provides a unique opportunity to study stem cell biology due to the well-defined hierarchy of blood cell production. Hematopoietic stem cells (HSCs) possess both self-renewal capabilities and full lineage potential for life-long maintenance of mature blood cells. The importance of understanding the regulation of this complex, highly coordinated process is accentuated by the role of aberrant HSC function in disease. Best understood in chronic and acute myeloid leukemias, leukemic stem cells (LSCs) arise from normal hematopoietic stem or progenitor cells and are capable of propagating the tumor. Epigenetic regulation of normal hematopoiesis is implicated by unaltered DNA sequences during lineage-specific differentiation, and recent evidence supports a role for DNA methylation changes in regulation of normal and malignant hematopoiesis. This work aims to better understand the epigenetic and transcriptional programs that regulate normal hematopoietic development as well as the molecular mechanisms that are involved in chronic myeloid leukemia (CML) leukemogenesis.

To begin our study, we performed genome-wide transcriptome analysis of highly refined CML and normal stem and progenitor cell populations. The persistence of LSCs in CML despite tyrosine kinase inhibition may explain patient relapse. We explored the transcriptional changes in CML LSCs to identify novel targets for the eradication of these cells while sparing normal HSCs. We identified genes that were differentially expressed in CML versus normal stem and progenitor cells and nominated cell surface genes that represent potential therapeutic targets. Further analyses of the LSCs revealed dysregulation of normal cellular processes, including downregulation of pro-

differentiation and TGF- β /BMP signaling pathways; upregulation of oxidative metabolism and DNA repair pathways; and activation of multiple oncogenes. These data represent an important resource for understanding the molecular changes in CML LSCs, which may be exploited to develop novel therapies for eradication of these cells and to achieve cure.

In order to investigate the epigenetic regulation of hematopoiesis, we utilized genome-wide gene expression data to specifically analyze transcriptional changes in hematopoietic stem and progenitor cells (HSPCs) from healthy bone marrow donors. We identified known epigenetic factors that were differentially expressed in HSPCs, including genes previously implicated in the regulation of HSC maintenance and lineage commitment programs. One gene, UHRF1, is a known essential cofactor in DNA methylation maintenance. UHRF1 also binds histone modifications and recruits chromatin modifying proteins to hemimethylated DNA, bridging both major forms of epigenetic control in cells. We generated an inducible, conditional knockout mouse model in order to explore the functional role of UHRF1 in hematopoietic development. We found that UHRF1 expression is indispensable for HSC function and propose that its role in lymphoid development may vary with degree of differentiation. These observations confirm that genes involved in epigenetic regulatory mechanisms are critical mediators of normal hematopoietic developmental programs.

Thesis Readers:

Mentor: William G. Nelson

Co-Mentor: Srinivasan Yegnasubramanian

DEDICATION

For Brian, my brother and the first Dr. Gucwa:

Thank you for paving the way.

ACKNOWLEDGEMENTS

I am fortunate to have an immense network of colleagues, friends, and family without which the completion of my Ph.D. would not have been possible. I truly hope that I have expressed even a fraction of my gratitude and made each of you feel appreciated along the way.

I owe much of my success to my thesis advisors, Drs. William G. Nelson and Srinivasan Yegnashubramanian. The N/Y lab was exactly the home I needed to learn and grow as a scientist. Vasana, the care you have for your students and the respect with which you treat your colleagues fosters an environment where intelligent, careful, and ingenious scientific research thrives. You have always had my best interest at heart, and I am eternally grateful for the innumerable times you believed in me when I could not believe in myself. You have an innate ability to see the unique value within each of your students and provide them with the necessary tools to reach their full potential. This and your enduring passion for science are what make you, far and away, an exceptional mentor. I am lucky to have had your guidance and support during this most formative time in my career.

I would also like to thank the members of my thesis committee, including committee chair Alan D. Friedman and my fellow co-authors, Jonathan Gerber and Gabriel Ghiaur, for contributing your expertise and valuable insights to my project. I owe a debt of gratitude to the Cellular and Molecular Medicine graduate program, especially director Rajini Rao and administrative coordinators, Colleen Graham and Leslie Lichter. I greatly appreciate your patience and support throughout my training.

I am particularly grateful for my fellow N/Y lab colleagues for contributing to such a pleasant and intellectually stimulating work environment. Thank you to Michael Haffner, Nicki Castagna, Jianyong Liu, Sunil Gangadharan, Jonathan Coulter, and Ruchama Steinberg, as well as recent graduates, Drs. Dave Walker, Nick Wyhs, Melody Tsui, Debika Biswal, and Chris Weier. I will always have fond memories of my times spent with the “night crew” – David Esopi, Ajay Vaghasia, Hugh Giovinazzo, and Kunhwa Kim. Thank you for bringing a little light to our nights together in lab.

During my time in Baltimore, I was lucky enough to meet a few people who gifted me their friendship and made this experience all the more valuable. Among those are my fellow CMM classmates. I am honored to have belonged to and worked alongside such an elite group of young scientists. In particular, I am grateful to Lauren Suarez who, in recent years, has been by my side to lend a shoulder to lean on or pick me up when I needed. I am proud that we’ve finally crossed the finish line and that we were able to do it together. To Megan and Young, thank you for providing an escape from reality at least once a week for the past 5 years. One person who has proven themselves invaluable to my life in Baltimore is my friend, neighbor, and second mother, Kate Burnett. I am lucky to know such a kind, generous, and optimistic soul as you. You are eternally loyal and bring light and happiness to all those who are lucky enough to call you a friend.

I cannot forget my friends who have been with me throughout all stages of my education – Marghi, Meghan, Katie, Sarah, and Colleen. From early on, you set a high standard for friendship that has been matched by few. To Vicki and Kathy, thank you for riding along with me through the many ups and downs over the past 15+ years. Your devoted friendship has given me the strength to stand more times than you may know.

As independent and successful women in your own careers, I admire your perseverance in accomplishing each goal you set for yourselves. I will continue to look to you both for inspiration as I begin this next stage in my career.

Most importantly, I would like to thank my family – my parents, Bill and Jan, and my brother, Brian – for being the solid foundation on which all of my life’s achievements have been built. Your unconditional love and support has, undoubtedly, driven my success in achieving this doctoral degree. For the countless sacrifices you have made, I love you and thank you.

TABLE OF CONTENTS

ABSTRACT	ii
DEDICATION	iv
ACKNOWLEDGEMENTS	v
TABLE OF CONTENTS	viii
LIST OF TABLES AND FIGURES	x
CHAPTER 1: INTRODUCTION	1
Hematopoietic Stem Cells and Identification	2
DNA Methylation in Hematopoiesis and Hematologic Malignancies	4
Objectives	5
CHAPTER 2: GENOME-WIDE COMPARISON OF THE TRANSCRIPTS OF HIGHLY ENRICHED NORMAL AND CHRONIC MYELOID LEUKEMIA STEM AND PROGENITOR CELL POPULATIONS	6
Introduction	7
Methods	8
Results	12
Discussion	18
Acknowledgements	22
Tables and Figures	23
Table 1. Plasma Membrane-Associated Genes that are Differentially Expressed in CML versus Normal Stem Cells	23
Figure 2.1. Global gene expression patterns in CML and normal stem and progenitor populations.	24
Figure 2.2. Differentially expressed genes between CML and normal stem and progenitor cells.	26
Figure 2.3. Altered cellular functions and pathways in CML LSCs compared to normal HSCs.	28
Figure 2.4. TGF-beta signaling pathway activity is altered in CML LSCs.	30
Figure 2.5. Exon-level analysis reveals evidence of alternative splicing in CML LSCs.....	32
CHAPTER 3: THE EPIGENETIC REGULATOR UHRF1 IN NORMAL HEMATOPOIESIS	33
Introduction	34
Methods	35
Results	40
Discussion	45

Acknowledgements.....	47
Tables and Figures	48
Figure 3.1. Gene expression changes of epigenetic regulatory factors involved in hematopoietic stem to progenitor cell differentiation.....	48
Figure 3.2. Induced conditional deletion of UHRF1 in the hematopoietic system.....	49
Figure 3.3. Conditional deletion of UHRF1 induces rapid lethality with pancytopenia and diminished bone marrow cellularity.....	51
Figure 3.4. Defective HSPC compartment in UHRF1 KO mice.	52
Figure 3.5. Reduced peripheral blood engraftment in UHRF1 KO competitive transplant model.....	54
Figure 3.6. Survival of a lymphoid committed population in UHRF1 KO competitive transplant model.....	57
CHAPTER 4: CONCLUSIONS AND FUTURE DIRECTIONS	58
REFERENCES	61
CURRICULUM VITAE.....	68

LIST OF TABLES AND FIGURES

Table 1. Plasma Membrane-Associated Genes that are Differentially Expressed in CML versus Normal Stem Cells.....	23
Figure 2.1. Global gene expression patterns in CML and normal stem and progenitor populations.....	24
Figure 2.2. Differentially expressed genes between CML and normal stem and progenitor cells.....	26
Figure 2.3. Altered cellular functions and pathways in CML LSCs compared to normal HSCs.	28
Figure 2.4. TGF-beta signaling pathway activity is altered in CML LSCs.	30
Figure 2.5. Exon-level analysis reveals evidence of alternative splicing in CML LSCs..	32
Figure 3.1. Gene expression changes of epigenetic regulatory factors involved in hematopoietic stem to progenitor cell differentiation.	48
Figure 3.2. Induced conditional deletion of UHRF1 in the hematopoietic system.....	49
Figure 3.3. Conditional deletion of UHRF1 induces rapid lethality with pancytopenia and diminished bone marrow cellularity.	51
Figure 3.4. Defective HSPC compartment in UHRF1 KO mice.	52
Figure 3.5. Reduced peripheral blood engraftment in UHRF1 KO competitive transplant model.....	54
Figure 3.6. Survival of a lymphoid committed population in UHRF1 KO competitive transplant model.....	57

CHAPTER 1: INTRODUCTION

Hematopoietic Stem Cells and Identification

Hematopoiesis is the process by which all mature blood cells are made and initiates from the hematopoietic stem cell (HSC). HSCs are multipotent and maintain the unique ability both to differentiate and self-renew¹. HSCs were one of the first identified somatic stem cells and are now easily isolated and tracked by well-defined cell surface markers^{2,3}. The first positive marker identified to enrich for cells possessing in vitro stem characteristics was the CD34 antigen⁴. CD38 expression was found to further refine this stem population, with CD34⁺CD38⁻ cells being highly enriched for NOD-SCID repopulating cells⁵. More recently, fluorescent cell staining methods have been developed to exploit the elevated expression levels of cytosolic ALDH in HSCs⁶.

In mice, FACS analysis of cell-surface markers is used to identify stem and progenitor cells of different developmental stages throughout the hematopoietic hierarchy⁷. The most mature cells in mouse bone marrow are defined by lineage markers, most commonly B220, CD3, Mac-1, Gr-1, and Ter-119, although Mac-1 has also been shown to be expressed on active cycling HSCs⁸ and is often omitted from mature lineage panels in mouse models where HSC quiescence may be perturbed. The first step in enrichment of bulk hematopoietic stem and progenitor (HSPC) populations is selection of lineage negative (Lin⁻) cells, followed by positive selection for Sca-1 and c-Kit expression to identify a bulk HSC population (LSK; Lin⁻Sca⁺Kit⁺) that includes stem and multipotent progenitor (MPP) cells. The LSK population can be further refined for long-term repopulating cells (or LT-HSCs) based on CD34 and FLT3⁹ or CD48 and CD150¹⁰ expression, as well as Hoechst dye efflux¹¹. Although the exact phenotype of the most primitive long-term repopulating cell has yet to reach a consensus, lymphoid

progenitors are classically distinguished by IL7RA expression, where the common lymphoid progenitor (CLPs) is Lin-Sca^{mid}Kit^{mid}IL7Ra+, while myeloid progenitors (MPs) are Lin-Sca-Kit+IL7Ra-. The MP bulk population can be further refined by CD34 and FcγRII/III (CD16/32) to identify common myeloid progenitors (CMP; CD34+CD16/32-), megakaryocyte-erythrocyte progenitors (MEP; CD34-CD16/32-) and granulocyte-macrophage progenitors (GMP;CD34+CD16/32+).

The gold-standard by which murine HSC function is defined is the long-term competitive repopulation assay. This allows for the identification of a primitive cell with the ability to repopulate all mature lineages in the peripheral blood of lethally irradiated recipient mice relative to WT competitor bone marrow¹². The success of this assay is dependent on the ability to distinguish the origin of transplanted marrow and is made possible by the availability of mice with congenic CD45 alleles. CD45 is a pan-leukocyte marker and is present on all hematopoietic cells in murine bone marrow as well as all differentiated cells in peripheral blood, with the exception of erythrocytes and platelets. In utilizing these markers, hematopoiesis resulting from CD45.2 donor marrow can be distinguished from the contribution of competitor CD45.1 marrow to peripheral blood repopulation, and percent chimerism and multi-lineage repopulation can be quantified. At 4 weeks following transplantation, repopulation of peripheral blood is maintained by a short-term repopulating cell, or bone marrow progenitor. Only after 16 weeks can the contribution of LT-HSCs to peripheral blood lineages be assessed in order to define the multi-lineage reconstitution capacity of the stem cell.

DNA Methylation in Hematopoiesis and Hematologic Malignancies

DNA methylation is a dynamic epigenetic modification necessary for gene regulation without specifically altering DNA sequences. Methylation of CpG dinucleotides is controlled by DNA methyltransferases (DNMTs)¹³. Changes in DNA methylation have been shown to be important in stem cell differentiation processes¹⁴, including lineage-commitment decisions of hematopoietic progenitor cells¹⁵. DNMT1 deficient mice were found to have reduced HSC self-renewal and impaired lymphoid differentiation but normal myeloerythroid development¹⁶. Recent studies utilizing genome-wide DNA methylation profiling techniques in both mouse and human have begun to elucidate possible genes and pathways involved in lineage commitment^{15,17}. However, these studies were limited to more downstream commitments by hematopoietic progenitors or heterogeneous bulk CD34+ populations. Primitive populations comprised of exclusively purified HSCs need to be examined at the whole-genome level to better understand epigenetic regulation of stem cell function.

Altered DNA methylation is a hallmark of cancer, including hematologic malignancies. Indeed, mice deficient in DNMT1 failed to induce leukemia upon transduction with leukemic fusion protein MLL-AF9¹⁶. Promoter hypermethylation was found to be a frequent event in AML with further increased methylation at relapse¹⁸. Additionally, examination of DNA methylation profiles in 344 AML patients allowed classification into 16 subtypes, each with a distinct methylation signature different from normal hematopoietic cells¹⁹. Together, these data implicate aberrant DNA methylation in leukemogenesis. In support of this, DNMT inhibitors have demonstrated clinical efficacy in myelodysplastic syndrome and acute leukemias²⁰. More recently, somatic

mutations in epigenetic modifying genes, such as *DNMT3A*, *TET2*, *IDH1/2*, *EZH2*, *MLL1*, and *ASXL1*, have been identified in hematologic malignancies²¹ and provide an explanation for altered epigenetic patterns in these disorders. Moreover, characterizing these genetic alterations in the context of patient outcomes may inform risk stratification and have important therapeutic implications²².

Objectives

We hypothesize that analysis of genome-wide gene expression data from normal and leukemic stem and progenitor populations can explain the molecular mechanisms regulating normal HSC function and leukemic transformation. We aim to first: understand the molecular changes in chronic phase CML LSCs, which may be exploited to develop novel therapies for eradication of these cells and to achieve cure, and second: investigate the influence of epigenetic modifying genes on normal hematopoietic development. To address these aims, we will explore differential expression patterns in normal and leukemic stem cell populations to identify unique cell surface markers that are selectively displayed on the CML LSC. Further analysis of global expression patterns will highlight mechanisms involved in the persistence of CML LSCs. Additionally, we will explore differential expression in epigenetic regulatory pathway components observed in normal HSPCs. Finally, we will use a murine model to understand the influence of the DNA methylation modifying gene, *UHRF1*, on normal hematopoietic differentiation.

**CHAPTER 2: GENOME-WIDE COMPARISON OF THE TRANSCRIPTS OF
HIGHLY ENRICHED NORMAL AND CHRONIC MYELOID LEUKEMIA
STEM AND PROGENITOR CELL POPULATIONS¹**

¹ Reprinted from *Oncotarget*. 2013;4(5):715-728. Gucwa JL, Gerber JM, Esopi D, Gurel M, Haffner MC, Vala M, Nelson WG, Jones RJ, Yegnasubramanian S. Genome-wide comparison of the transcriptomes of highly enriched normal and chronic myeloid leukemia stem and progenitor cell populations. Supplemental material can be found at <http://www.impactjournals.com/oncotarget>.

Introduction

Despite the significant improvement in survival rates of chronic phase (CP) chronic myeloid leukemia (CML) patients made possible by tyrosine kinase inhibitor (TKI) therapy, cures outside of allogeneic blood or marrow transplantation are rare²³⁻²⁶. This appears to be due to the resistance of leukemia stem cells (LSCs) in CML to the proapoptotic effects of TKI agents²⁷⁻³⁰. Accordingly, most CML patients who discontinue TKIs while in molecular remission eventually relapse³¹. Moreover, for most of the TKI-induced cytogenetic remissions that remain durable at least 7 years, CML LSCs in these patients can still acquire additional mutations with progression to blast crisis (BC)³². Thus, there remains a clear need to identify novel molecular targets specific to the CML LSCs³³.

The precise mechanisms of CML LSC resistance to TKIs are not fully defined. CML LSCs appear to share many biological properties with their normal counterparts^{28,34} that probably limit the effectiveness of therapeutic strategies targeting BCR-ABL signaling. Hematopoietic stem cells (HSCs) are largely quiescent and normally express high levels of the multidrug resistance-1 gene³⁵, two factors that may limit the cellular uptake of imatinib³⁶. Moreover, BCR-ABL expression appears to be required for the survival of CML progenitors but not CML LSCs, where the *BCR-ABL* gene can be silent likely because HSCs already are long-lived and self-renew^{34,37}.

Biologic studies on LSCs have been hampered by the relative rarity of these cells, as well as the lack of a consensus on their exact phenotype. LSCs are often phenotypically defined as simply the CD34⁺ leukemia cells or, more recently, the more enriched CD34⁺CD38⁻ subset, but even the CD34⁺CD38⁻ cells are a heterogeneous

population of which the LSCs constitute only a fraction^{34,38}. Normal CD34⁺CD38⁻ cells can be further refined for HSCs based on low side scatter and high aldehyde dehydrogenase (ALDH) 1 activity^{39,40}. As few as 1,000 normal CD34⁺CD38⁻ALDH^{high} cells will reproducibly engraft NOD/SCID-IL2R^{null} (NSG) mice⁴⁰. The major biologic function of the ALDH1 family, also known as the retinaldehyde dehydrogenases, is the biosynthesis of retinoic acid, but they also participate in the detoxification of a variety of compounds such as ethanol and active metabolites of cyclophosphamide⁴¹. We previously reported that high ALDH expression also can distinguish CML cells capable of engrafting NSG mice (i.e. CML LSCs) from more differentiated CML progenitors within the CML CD34⁺CD38⁻ population⁴². Importantly, expression of putative therapeutic targets by CML progenitor cells was not necessarily representative of that in the CML LSCs⁴², highlighting the need to search for new targets in refined LSC populations. Here, we report a comprehensive transcriptional profile of CML LSCs as compared to normal HSCs and identify unique cell surface molecules and mechanistic pathways that may serve as potential CML LSC targets.

Methods

Patient and normal donor bone marrow specimens, enrichment of stem and progenitor cell populations, and nucleic acid extraction

Bone marrow was obtained from 5 patients with newly-diagnosed and untreated CP CML, as well as from 5 healthy bone marrow donors. Informed consent was obtained from all patients and healthy donors prior to sample collection in accordance with the Declaration of Helsinki, under a research protocol approved by the Johns Hopkins Institutional Review Board. CD34⁺CD38⁻ALDH^{high} stem cells and CD34⁺CD38⁺

progenitor cells were collected from each marrow specimen as described previously⁴². Briefly, CD34⁺ cells were selected using Miltenyi Biotec (Auburn, CA) microbeads (binding the class II CD34 epitope) followed by column enrichment per the manufacturer's recommendations. These cells were then stained with Aldefluor (Aldagen, Durham, NC) to assess ALDH activity, phycoerythrin-conjugated anti-CD34 antibodies (binding the class III CD34 epitope), and allophycocyanin-conjugated anti-CD38 antibodies (BD Biosciences, San Jose, CA), and sorted using a MoFlo cell sorter (Beckman Coulter) into CD34⁺CD38⁻ALDH^{high} and CD34⁺CD38⁺ fractions. DNA and RNA were extracted from at least 50,000 cells from each population using the All-prep micro kit (Qiagen, Valencia, CA, USA).

Fluorescence in situ hybridization (FISH)

Isolation of leukemic cells was confirmed by FISH for *BCR-ABL* on cytopins of each sorted cell fraction, fixed in 3:1 Methanol: Glacial Acetic acid (Sigma-Aldrich, St. Louis, MO, USA). FISH was performed by the Johns Hopkins Cytogenetics Core, using the Vysis LSI *BCR-ABL* Dual Color, Dual Fusion translocation probe (Abbot Molecular, Des Plaines, IL, USA) per manufacturer's instructions. Slides were analyzed on a fluorescence microscope with a triple-band pass filter for DAPI, Spectrum Orange, and Spectrum Green.

Gene expression microarrays and analysis

Total RNA from sorted cell populations was subjected to cDNA synthesis and linear amplification using the Ovation RNA Exon Module amplification system (NuGEN, San Carlos, CA) according to the manufacturer's protocols. The resulting material was then

fragmented and biotin-end-labeled using the Encore Biotin Module (NuGEN) and hybridized to Human Exon 1.0 ST whole genome gene expression microarrays (Affymetrix, Santa Clara, CA) according to the manufacturer's protocols at the Johns Hopkins Microarray facility. The microarray gene expression data was analyzed with Partek Genomic Suite software (<http://www.partek.com/partekgs>) using the exon array workflow with default conditions (data imported and normalized using \log_2 transformation, default RMA background correction and normalization of core meta-probe sets) unless otherwise specified. Gene expression summaries from the imported normalized intensity data was subjected to principal components analysis. Two-way analysis of variance (ANOVA) of gene summary data was performed to find differentially expressed genes between all cell populations, focusing on the contrasts between CML versus normal samples and CML CD34⁺CD38⁻ALDH^{high} versus normal CD34⁺CD38⁻ALDH^{high} populations. Genes with $|\log_2(\text{fold-change})| > 1$ and false discovery rate (FDR) of 0.05 were identified as significantly differentially expressed. A gene list specifically focusing on contrasts between CML and normal CD34⁺CD38⁻ALDH^{high} cells with $|\log_2(\text{fold-change})| > 1$ and false discovery rate (FDR) of 0.05 was uploaded to the Database for Annotation, Visualization, and Integrated Discovery (DAVID) v6.7 (<http://david.abcc.ncifcrf.gov/>) for functional annotation analyses^{43,44} of enriched gene ontology (GO) and KEGG pathway terms. Lists comprised of all arrayed genes with expression data from the CML versus normal CD34⁺CD38⁻ALDH^{high} comparison were subjected to gene-set enrichment analysis (GSEA), as described previously⁴⁵⁻⁴⁷, or directly uploaded into Ingenuity Pathway Analysis (IPA) software (Ingenuity® Systems, June 2012, www.ingenuity.com). For GSEA, all GO and KEGG

terms with a q-value less than 0.01 were considered significant. Core analysis was run in IPA utilizing all default settings, with exception of the Human Exon 1.0 ST array as the reference gene set. This analysis generated a list of potential upstream transcriptional regulators and predicted the activity of each by calculation of overlap p-value using a Fisher's Exact test and the activation Z-score as described (Ingenuity® Systems, www.ingenuity.com). Calculations were based on known interactions between the predicted upstream transcriptional regulators and their downstream target gene set according to the Ingenuity® Knowledge Base and measured expression changes in the array data set. Upstream regulators with $|z\text{-score}| > 2.00$ were nominated as significant, with a positive Z-score representing activation and a negative value, inhibition. The list of upstream regulators and activation z-score values were also utilized to assign the activation state of each component of the TGF- β pathway, which was defined using the IPA and KEGG pathway map data (<http://www.genome.jp/kegg/pathway.html>). The raw and normalized data are available from the Gene Expression Omnibus (GEO) with accession number GSE43754. For alternative transcript analysis, exon level microarray data from the CML and normal CD34⁺CD38⁻ALDH^{high} RNA was subjected to ANOVA analysis using the default conditions on the Partek alternative transcript workflow. Genes with alternative transcript p-value < 0.01 were subjected to analysis with DAVID v.6.7 as described above. For each probeset within a gene, the $\log_2(\text{normalized intensities})$ for each sample was adjusted by the average normalized intensity of the normal samples. The resulting mean and standard deviation for CML or normal samples was plotted according to probeset number, assigned 5'-3', for each representative gene.

Real-time reverse transcriptase polymerase chain reaction

Excess extracted RNA from patient samples was used to synthesize cDNA using SuperScript® III Reverse Transcriptase (RT) (Invitrogen, Carlsbad, CA). Newly synthesized cDNA from unamplified RNA or excess amplified cDNA prior to labeling and array hybridization from each CML and normal patient sample was used to validate array results by quantitative RT-PCR of *GAS2*, *DPP4*, *CDH2*, *IL2RA*, *GAPDH* and *ACTB* using the iQ Supermix (Bio-Rad, Hercules, CA) and gene-specific TaqMan® assays (Life Technologies Co., Carlsbad, CA). The relative amount of the gene of interest was determined using the $\Delta\Delta C_t$ method, relative to the average expression of all samples for that gene and *GAPDH* expression for *GAS2*, *DPP4*, and *CDH2* or *ACTB* for *IL2RA*. Quantitative RT-PCR results from amplified starting material or SuperScript® III converted unamplified cDNA were compared for the gene *IL2RA* and showed consistent results. The remaining genes were verified using amplified starting material only. All quantitative PCR experiments were done in duplicate.

Results

Identification of potential targets that can distinguish CML LSCs from normal HSCs

In order to characterize the expression profile of CP CML LSCs and identify potential therapeutic targets unique to this population, we sorted $CD34^+CD38^+$ and $CD34^+CD38^-ALDH^{high}$ cells to obtain highly enriched populations of progenitor and stem cells, respectively, from bone marrow of both healthy donors and CP CML patients (Figure 1A; Supplementary Table 1). As already discussed, HSCs are enriched in the $CD34^+CD38^-ALDH^{high}$ cells^{39,40}, and these cells contain few of the more differentiated

colony-forming unit or progenitor cells, which are enriched in the CD34⁺CD38⁺ cell fraction⁴⁸. Likewise, CD34⁺CD38⁻ALDH^{high} cells show enrichment for CML LSCs with enhanced engraftment capabilities in immune deficient mice compared to the remaining CD34⁺CD38⁻ cells⁴². Whole transcriptome profiling of each population was carried out by microarray analysis using an Affymetrix Human Exon 1.0 ST array, allowing measurement of differential gene expression and analysis of alternative transcripts. Principal components analysis of the gene-level data revealed distinct clustering of the four populations and showed that global gene expression patterns between the normal and CML CD34⁺CD38⁻ALDH^{high} cells are closer to each other than normal are to their matched CD34⁺CD38⁺ cells (Figure 1B). Furthermore, the CML subset displayed greater variability in the gene expression patterns than their normal counterparts. Part of this variability in the CML CD34⁺CD38⁻ALDH^{high} fraction could be accounted for by the presence of residual *BCR-ABL* negative normal HSC in this cell population; the two subjects with the highest fraction of residual normal HSC clustered most closely with the normal HSC (Figure 1; Supplementary Table 1).

Although global gene expression patterns in the CML and normal CD34⁺CD38⁻ALDH^{high} cells were fairly similar, gene-level analysis allowed us to identify several genes with significant differential expression that may serve as therapeutic targets. Using ANOVA, we identified genes that were significantly differentially expressed between all CML vs. normal samples, regardless of sorted population, and also those that were significantly differentially expressed specifically between CD34⁺CD38⁻ALDH^{high} cell populations of CML and normal samples (FDR = 0.05, $|\log_2(\text{Fold Change})| > 1$). A total of 97 genes were identified through this analysis and a heatmap was created showing the

expression patterns of each gene across the four cell populations (Figure 2A). Notably, expression of this gene set was able to distinguish CML stem and progenitor cells from their normal counterparts by hierarchical clustering. Thirty-one transcripts were found to be upregulated in CML CD34⁺CD38⁻ALDH^{high} cells compared to normal CD34⁺CD38⁻ALDH^{high} or CD34⁺CD38⁺ cells (Figure 2A), representing selective putative CML stem cell targets. These included *BLM*, *FAS*, *KYNU*, *NCF4*, *PTPRD*, *RAB31*, *SCD*, *ABHD10*, and *HPGDS*, genes known to be involved in key cell signaling and metabolic pathways. The most upregulated gene selectively expressed on CML CD34⁺CD38⁻ALDH^{high} when compared to their normal counterparts was *GAS2* ($p = 5.96 \times 10^{-11}$, average fold change = 23.5; Figure 2B). To further analyze our list of potential LSC-specific targets, functional annotation by the Database for Annotation, Visualization, and Integrated Discovery (DAVID) of genes differentially expressed on the CML versus normal CD34⁺CD38⁻ALDH^{high} cells (FDR = 0.05, $|\log_2(\text{Fold Change})| > 1$); represented by (●) in Figure 2) was carried out and highlighted several plasma membrane-associated genes (GO:0044459, Plasma Membrane Part), including the most up- and down-regulated genes, *DPP4* and *CDH2*, respectively (Table 1). From this list, *DPP4*, *IL2RA*, *RAB31*, *PTPRD*, *CACNA1D*, *IL1RAP*, *SLC4A4*, and *KCNK5* were upregulated in the CML CD34⁺CD38⁻ALDH^{high} population and exhibit a cell surface protein localization. Microarray expression levels were verified by quantitative RT-PCR for a few select interesting genes (Figure 2B). Microarray intensity values were highly correlated with relative expression levels determined by quantitative RT-PCR analysis.

Dysregulation of proliferation, differentiation and molecular pathways in CML LSCs

Characterization of the molecular mechanisms underlying malignant transformation of the normal HSCs to LSCs may aid in target discovery by uncovering pathways critical to initiation, self-renewal, and survival of the CML LSCs. Gene set enrichment analysis (GSEA)⁴⁵⁻⁴⁷ of all Gene Ontology (GO)⁴⁹ and KEGG^{50,51} gene sets was used to identify pathways that show significant and coordinate up or down regulation of pathway components using all genes interrogated by the microarray platform. Significant terms with a q-value (multiple hypothesis testing corrected p-value) less than 0.01 indicated upregulated and downregulated gene sets that are putatively important to LSC biology; these terms were categorized by cellular functions (Supplementary Table 2 shows all significant gene sets). The top three GO and KEGG terms for each category are shown in Figure 3. Gene sets that were upregulated in CML versus normal CD34⁺CD38⁻ALDH^{high} were involved in cell cycle and proliferation, mRNA processing, translation, DNA repair, oxidative metabolism, protein processing, immune response, and metabolic processes. Key downregulated gene sets in the CML CD34⁺CD38⁻ALDH^{high} cells were associated with the cell surface and extracellular matrix, differentiation and developmental programs, cellular response to stimuli, and TGF- β and BMP signaling pathways.

One challenge in interpreting the results of the gene-set enrichment analyses is that, for many molecular pathways, there may be a de-coupling between the transcriptional levels of the pathway components and the steady-state downstream output of the pathways, often due to complex feedback mechanisms. Therefore, it would be useful to directly examine whether the steady state transcriptional output of the pathway

is consistent with overall pathway activation or inactivation. To carry out this type of vectoral analysis, we used the IPA Upstream Regulator analysis, which integrates literature-based information on the relationship between a given candidate upstream regulator and the direction of its influence on the transcriptional level of each of its downstream targets with the differential expression data generated in a given experiment to predict the activation (or inactivation) state of the upstream regulator (Ingenuity® Systems, www.ingenuity.com). Each candidate upstream regulator was assigned a Z-score, representing the confidence with which the regulator is activated or inactivated, with high positive Z-scores representing activation and high negative Z-scores representing inactivation of the function of each upstream regulator. We applied this analysis to our gene expression data from CML and normal CD34⁺CD38⁻ALDH^{high} cells. A Z-score greater than 2 or less than -2 was considered to be activated or inhibited, respectively, in CML relative to normal CD34⁺CD38⁻ALDH^{high} cells (Supplementary Table 3 shows all significant molecules, excluding all “chemical”-related upstream molecule types). The top upstream regulator molecules showed activation of several oncogenes, such as *MYC*, *TBX2*, and *CCND1*, and inflammatory chemokines, such as *CCL2* and *CXCL2*, and inhibition of several tumor suppressors, including *TP53* and *CDKN2A* (Figure 4A, excluding “chemical”-related and “other” upstream molecule types; Supplementary Table 3). Consistent with downregulation of the TGF-β/BMP pathways as observed by GSEA, we observed a strong inhibition of the transcriptional output of the TGF-β and BMP signaling pathway (Figure 4B), with inhibition of pathway agonists including *TGFB1* itself, *BMP2*, *GDF2*, and activation of pathway antagonists, such as *SMAD7* and *NOG* (Figure 4A,B).

Alternative transcriptional isoforms in CML LSCs

Gene sets associated with RNA processing and, more specifically, mRNA processing were shown by GSEA to be significantly differentially regulated in the CML compared to normal CD34⁺CD38⁻ALDH^{high} cells (Figure 3). We, therefore, examined the exon array data to explore differential exon usage in the CML versus normal CD34⁺CD38⁻ALDH^{high} cells. Evidence of alternative splicing, defined for a given gene as one or more exons displaying expression patterns different from the behavior of the other exons, was apparent in 236 genes (FDR = 0.01; Supplementary Table 4). The top two genes ranked by alternative splicing p-value that showed unique exon behavior were *CACNA1D* and *PDE4D* (Figure 5A). *CACNA1D* also was identified as a top upregulated gene in CML stem and/or progenitor populations compared to normal (Figure 2). This differential expression was probably due to extensive alterations in exon usage across the gene, whereas *PDE4D* displayed preferential expression of specific alternative transcript isoforms in CML CD34⁺CD38⁻ALDH^{high} cells compared to their normal counterparts. Functional annotation of this alternatively transcribed gene list by DAVID analysis was done to gain further insight into the biological processes affected by alternative exon usage/alternative splicing in CML CD34⁺CD38⁻ALDH^{high} cells. This analysis revealed that alternative transcripts in the CML CD34⁺CD38⁻ALDH^{high} cells, when compared to normal counterparts, were enriched in cellular proliferation genes, p53 signaling pathway, and kinase binding genes. There were 29 genes identified to be involved in regulation of cellular proliferation, including *MYCN* and *TIMELESS* (Figure 5Biii). Seven genes were involved in p53 signaling, including *CDKN1A*, which was also found

in the cell proliferation category, and *PERP* (Figure 5Bi). Twelve genes had kinase binding functions, including *MARCKS* and *DUSP12* (Figure 5Bii).

Discussion

LSCs appear to persist in most CML patients on TKIs, and the persistence of these cells remains a major obstacle to cure.^{27,29,31} We previously reported that ALDH expression enriched for CD34⁺CD38⁻ cells capable of engrafting NSG mice from normal marrow⁴⁰ as well as CML⁴², thus, presumably representing the primitive stem cell fractions in both. Moreover, expression of some putative targets by the CML LSCs differed significantly from that of the more prevalent progenitor cells⁴², highlighting the need to study refined LSC populations. Additionally, other CML antigens were expressed at comparable levels to normal stem/progenitor cells, suggesting a lack of leukemia-specificity and a high likelihood that therapies targeting these candidates might cause undue toxicity to normal hematopoiesis⁴².

We employed exon microarray technology to perform whole transcriptome analysis of highly enriched CP CML and normal stem and progenitor cell populations with the goal of identifying unique putative LSC targets. Interestingly, principal components analysis revealed that expression patterns were remarkably similar between the CD34⁺CD38⁻ALDH^{high} cells from CML patients and those from normal donors. In fact, the similarities were greater than those observed between the CML LSCs (CD34⁺CD38⁻ALDH^{high} cells) and the CML progenitors (CD34⁺CD38⁺ cells), underpinning the challenge in selectively targeting LSCs without injuring normal HSCs. Nonetheless, the comprehensive approach and highly refined populations utilized in this analysis allowed identification of important new putative LSC targets that were more

highly expressed by the CML LSC and/or progenitor cell fractions compared to normal stem/progenitor cell fractions.

A significant number of genes over-expressed in CML LSCs compared to their normal counterparts encoded cell surface proteins, including, *IL2R α* , *DPP4*, *PTPRD*, *CACNA1D*, *IL1RAP*, *SLC4A4*, and *KCNK5*. The surface location of these candidates may render them particularly vulnerable to targeting by immune-based strategies. *DPP4*, also known as CD26, encodes dipeptidyl peptidase 4, and is especially interesting as a possible target for LSC-directed therapy. One of the known targets of its peptidase cleavage activity is CXCL12⁵², and upregulation of DPP4 on the surface of CML LSCs may allow these cells to escape the homing/niche interactions imposed by the CXCL12/CXCR4 chemokine-receptor system⁵³, leading to dysregulated LSC growth and survival. Therefore, drugs capable of inhibiting the DPP4 dipeptidyl peptidase catalytic activity, which are currently FDA-approved for treatment of diabetes⁵⁴, may have utility in targeting CML LSCs. IL2RA is also a particularly attractive LSC target since multiple biologic agents directed against it are currently under clinical investigation⁵⁵. IL1RAP has been identified previously as a putative therapeutic stem cell-specific target in CML⁵⁶, as well as in acute myeloid leukemia (AML) and myelodysplastic syndrome (MDS) patients, with high expression correlating with poor overall survival in AML⁵⁷. Similarly, in this study, we identified *IL1RAP* upregulation on CML LSCs; the availability of IL-1 receptor antagonists or decoy receptors that are currently FDA-approved for the treatment of several inflammatory disorders⁵⁸ may allow effective targeting of the CML LSC. Among the other genes found to be upregulated in LSCs compared to normal HSCs, *BLM*, *KYNU*, *PTPRD*, *RAB31*, and *HPGDS* are known to

have enzymatic activities involved in key signaling and metabolic pathways; development of inhibitors of these enzymes may allow LSC targeting.

Taking advantage of the comprehensive coverage of the exon array platform, we also identified several genes that were dysregulated in LSCs at the level of alternative transcriptional isoforms and alternative exon usage. Interestingly genes showing alternative splicing were enriched in p53 signaling, protein kinase binding and cell proliferation. Therefore, alternative splicing may account in part for the increased cell proliferation, resistance to apoptosis, and dysregulated kinase signaling characteristic of CML⁵⁹. It is expected that these pathways and their components are susceptible to pharmacologic inhibition. Of particular interest, the cyclic-AMP specific phosphodiesterase, *PDE4D*, was found to be upregulated in CML LSCs compared to normal HSCs by preferential expression of a specific alternative transcript isoform. Likewise, the dual specificity phosphatase, *DUSP12*, and the voltage-dependent L-type calcium channel, *CACNA1D*, appear to become upregulated in CML LSCs via alternative exon usage. It is possible that alternative splicing of *DUSP12* in CML LSCs could underlie immunogenic responses that seem to correlate with improved survival after donor lymphocyte infusion⁶⁰. Although PDE4 inhibitors and L-type calcium channel blockers are available, development of isoform specific inhibitors may aid in CML LSC targeting. Therefore, such alternative transcription analyses could be used to identify functionally critical exons and their corresponding protein domains for development of targeted and immunomodulatory therapies.

Using these comprehensive transcriptome data, we were able to identify key pathways that were altered in the LSCs compared to normal HSCs. Consistent with

previous findings of Bruns et al ⁶¹, we observed upregulation of several pathways involved in cell proliferation/cell cycle, and downregulation of pathways involved in cell surface interactions, development, and differentiation. These pathway alterations may underlie the increased cell proliferation and resistance to apoptosis that are characteristic of CML and may also play a significant role in recognized resistance mechanisms of LSCs, such as dysregulation of niche interactions, cell cycle, survival, self-renewal, and metabolism. Interestingly, and somewhat unexpectedly, we also observed upregulation of pathways involved in oxidative metabolism, suggesting that LSCs may not be as metabolically quiescent as previously thought⁶². The accompanying upregulation of DNA repair pathways in the CML LSCs may indicate a requirement for guarding against DNA damage induced by a potential increase in production of reactive oxygen species during oxidative metabolism. Additionally, we identified a number of signaling pathways that showed evidence of activation in the LSCs. Particularly interesting are the targets with specific inhibitors already under clinical investigation, including a neutralizing monoclonal antibody to CCL2⁶³ and cyclin dependent kinase 4/6 inhibitors, inhibiting activation by partnering cyclin CCND1^{64,65}. Additionally, we found that the TGF- β /BMP pathway was coordinately downregulated in the CML LSC compared to normal HSC, and pathway antagonists, such as *SMAD7* were highly activated. The likely contribution of *SMAD7* activation to the observed TGF- β pathway inhibition in CML LSCs compared to normal HSCs and the current clinical investigation of antisense oligonucleotides for *SMAD7* inhibition in Crohn's disease⁶⁶ make it an attractive target for CML LSC-directed therapy. Although previous reports have shown that the TGF- β pathway is critical for CML LSC survival⁶⁷⁻⁶⁹, it also has been suggested that TGF- β has

a dual role in tumor progression, acting as a tumor suppressor in the very early stages of tumorigenesis^{70,71}.

We have developed an important resource for identifying the gene expression changes, pathway alterations, and alternative exon usage that can allow selective targeting of CP CML LSCs. Some of these targets, such as *IL2RA* and *DPP4*, may be amenable to immediate clinical translation with currently available therapies. While this work requires further functional validation and target credentialing, it offers the promise of LSC-targeted therapies, which may prove curative in CML while minimizing harm to normal hematopoiesis.

Acknowledgements

I would like to thank Jonathan Gerber and Milada Vala for bone marrow sample preparation and cell sorting experiments, David Esopi and Michael Haffner for microarray sample preparation and validation, and Meltem Gurel for gene set enrichment analysis. Special thank you to Jonathan Gerber and Srinivasan Yegnasubramanian for designing the study and providing valuable guidance in interpreting these results.

Tables and Figures

Table 1. Plasma Membrane-Associated Genes that are Differentially Expressed in CML versus Normal Stem Cells

Gene Symbol	Fold Change Expression*	P	Genomic Location†	Gene Name
<i>DPP4</i>	9.77	1.23E-06	2q24.3	dipeptidyl-peptidase 4
<i>IL2RA</i>	6.08	3.27E-07	10p15-p14	interleukin 2 receptor, alpha
<i>RAB31</i>	5.13	7.92E-06	18p11.3	RAB31, member RAS oncogene family
<i>PTPRD</i>	5.01	5.02E-06	9p23-p24.3	protein tyrosine phosphatase, receptor type, D
<i>CACNA1D</i>	3.53	8.39E-07	3p14.3	calcium channel, voltage-dependent, L type, alpha 1D subunit
<i>IL1RAP</i>	2.90	7.69E-05	3q28	interleukin 1 receptor accessory protein
<i>SLC4A4</i>	2.50	6.28E-05	4q21	solute carrier family 4, sodium bicarbonate cotransporter, member 4
<i>KCNK5</i>	2.06	5.58E-05	6p21	potassium channel, subfamily K, member 5
<i>CADPS2</i>	-2.29	2.74E-05	7q31.3	Ca ⁺⁺ -dependent secretion activator 2 GTP binding protein overexpressed in skeletal muscle
<i>GEM</i>	-2.52	1.58E-05	8q13-q21	muscle
<i>ANK3</i>	-2.87	1.35E-05	10q21	ankyrin 3, node of Ranvier (ankyrin G)
<i>PGM5</i>	-2.96	1.13E-04	9q13	phosphoglucomutase 5
<i>IGF1R</i>	-2.96	1.28E-05	15q26.3	insulin-like growth factor 1 receptor
<i>EMCN</i>	-3.12	4.91E-05	4q24	endomucin
<i>CNTN1</i>	-4.32	2.28E-05	12q11-q12	contactin 1
<i>PERP</i>	-4.41	1.31E-04	6q24	PERP, TP53 apoptosis effector
<i>CDH2</i>	-4.73	5.75E-07	18q11.2	cadherin 2, type 1, N-cadherin (neuronal)

Functional annotation results by DAVID are represented in the table, showing genes enriched for gene ontology term “Plasma Membrane Part” (GO:0044459).

*Calculated between CML and normal stem (CD34⁺ CD38⁻ ALDH^{high}) cell populations from five CML or normal marrow donors from log₂ transformed, default RMA background corrected array intensities. Positive values (red) indicate upregulation of gene in CML compared to normal, and negative values (blue) indicate downregulation in CML.

†Genomic coordinates refer to the human reference genome hg19 (GRCh37).

Figure 2.1

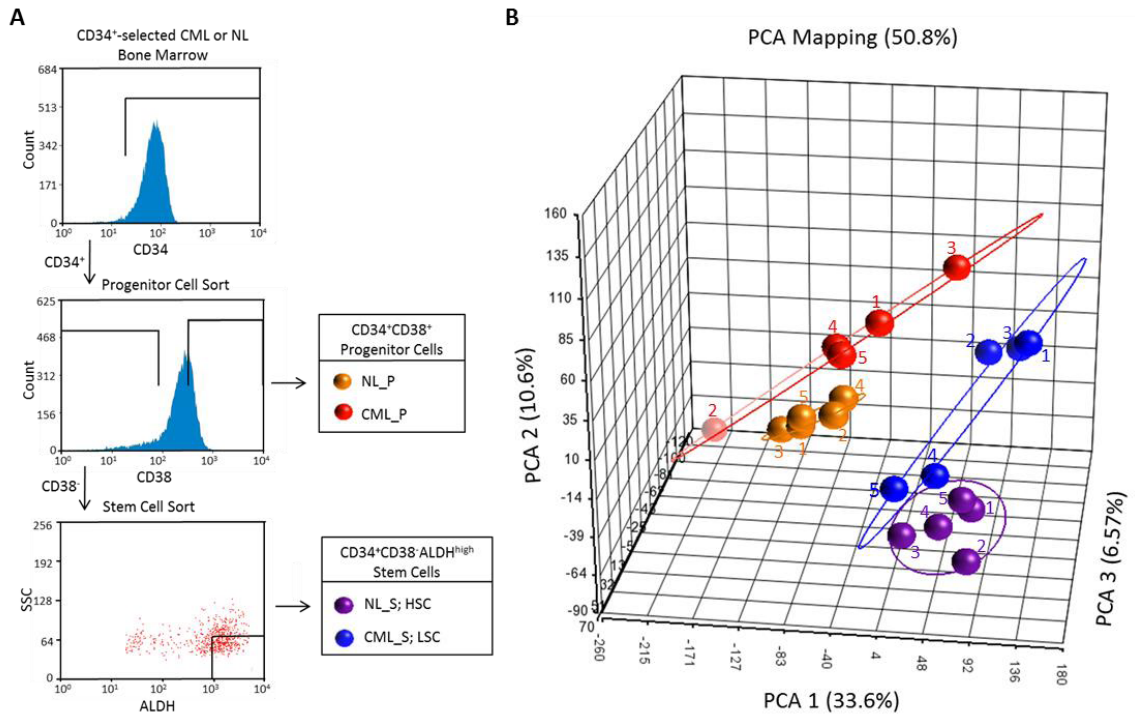


Figure 2.1. Global gene expression patterns in CML and normal stem and progenitor populations. (A) Cell sorting schematic for isolation of stem CD34⁺CD38⁻ALDH^{high} and CD34⁺CD38⁺ cells. A representative CML sample is shown. An analogous strategy was used to sort normal (NL) samples. (B) Principal components analyses (PCA) were done on microarray gene-level expression data for CML and normal CD34⁺CD38⁻ALDH^{high} and CD34⁺CD38⁺ cell populations. CML_S (blue symbols), chronic myeloid leukemic stem (CD34⁺CD38⁻ALDH^{high}) cells; CML_P (red symbols), chronic myeloid leukemic progenitor (CD34⁺CD38⁺) cells; NL_S (purple symbols), normal stem (CD34⁺CD38⁻ALDH^{high}) cells; NL_P (yellow symbols), normal progenitor (CD34⁺CD38⁺) cells. Sample IDs correspond to Supplementary Table 1.

Figure 2.2

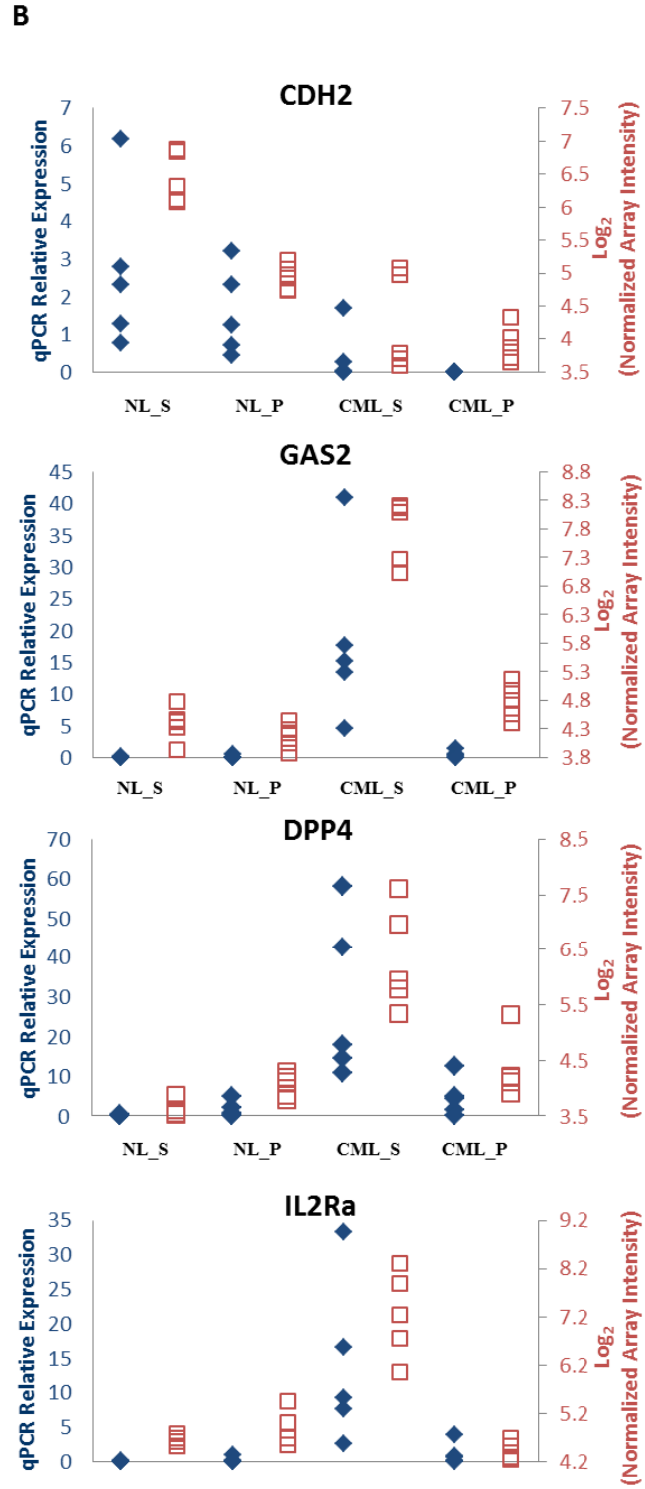
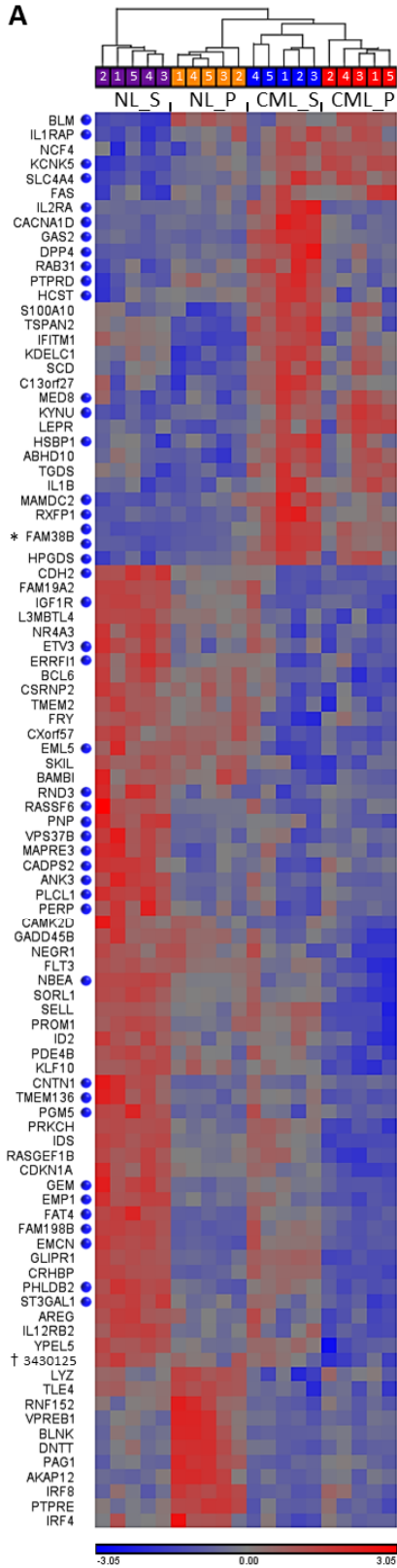


Figure 2.2. Differentially expressed genes between CML and normal stem and progenitor cells. CML_S, chronic myeloid leukemic stem ($CD34^+CD38^-ALDH^{high}$) cells; CML_P, chronic myeloid leukemic progenitor ($CD34^+CD38^+$) cells; NL_S, normal stem ($CD34^+CD38^-ALDH^{high}$) cells; NL_P, normal progenitor ($CD34^+CD38^+$) cells. A) Heatmap showing expression patterns of genes found by ANOVA to be differentially expressed between CML and normal $CD34^+CD38^-ALDH^{high}$ and $CD34^+CD38^+$ cells. Sample IDs correspond to Supplementary Table 1. Blue dots (●) represent genes differentially expressed in CML versus normal $CD34^+CD38^-ALDH^{high}$ cells with $FDR = 0.05$ and $|\log_2(\text{Fold Change})| > 1$. Upregulated and downregulated expression levels are indicated in red and blue, respectively. *FAM38B is represented by 2 separate Affymetrix transcript IDs (3798778; 3798829). †No gene name associated with Affymetrix transcript ID 3430125. B) Four candidate differentially expressed genes are shown. cDNA was prepared for each sample as described in Methods. To visualize quantitative RT-PCR (qPCR) results (blue axes labels, ◆), the relative amount of the gene of interest was determined using the $\Delta\Delta C_t$ method. Microarray expression was plotted using \log_2 transformed, default RMA background corrected array intensities (red axes labels, □).

Figure 2.3

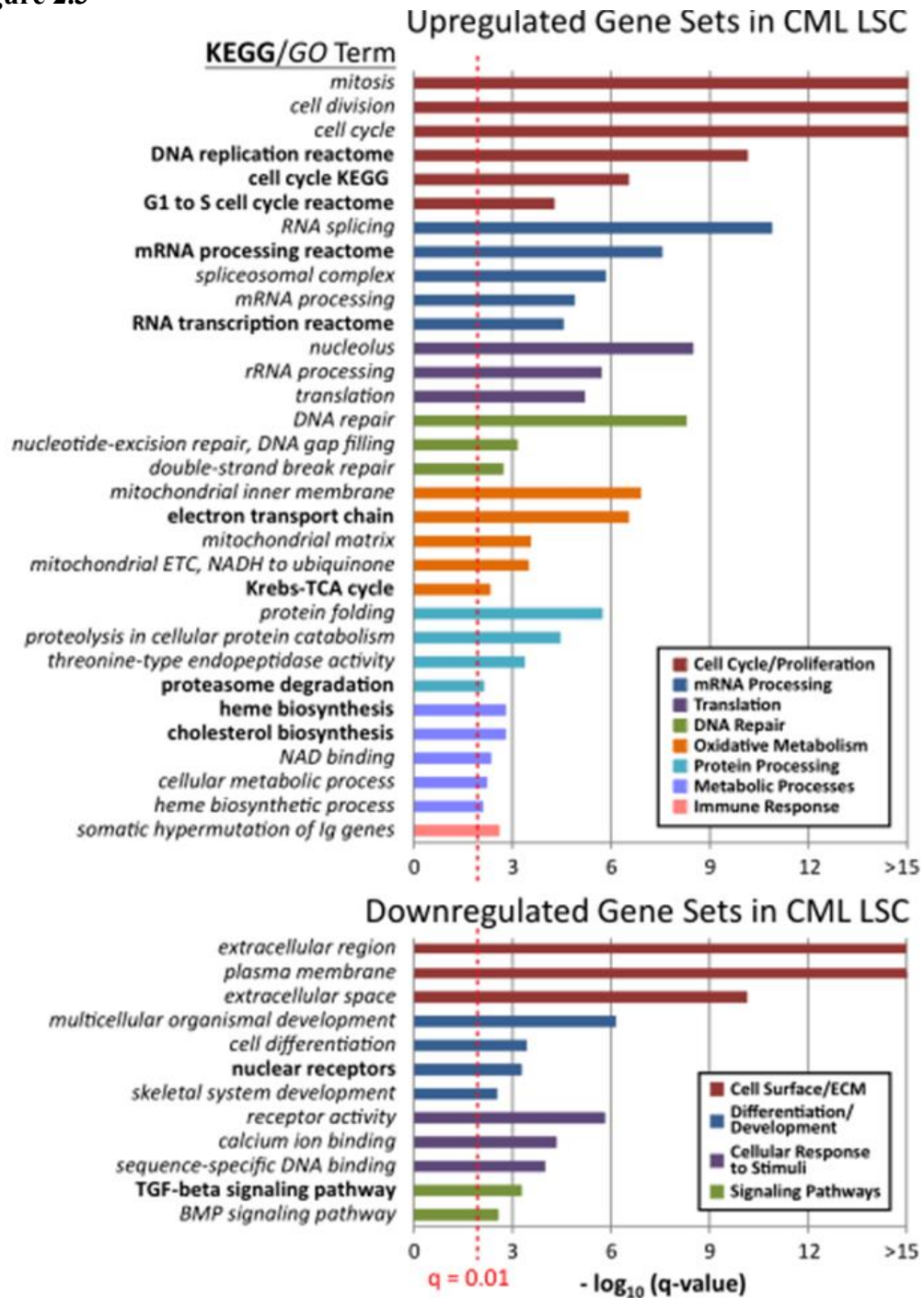
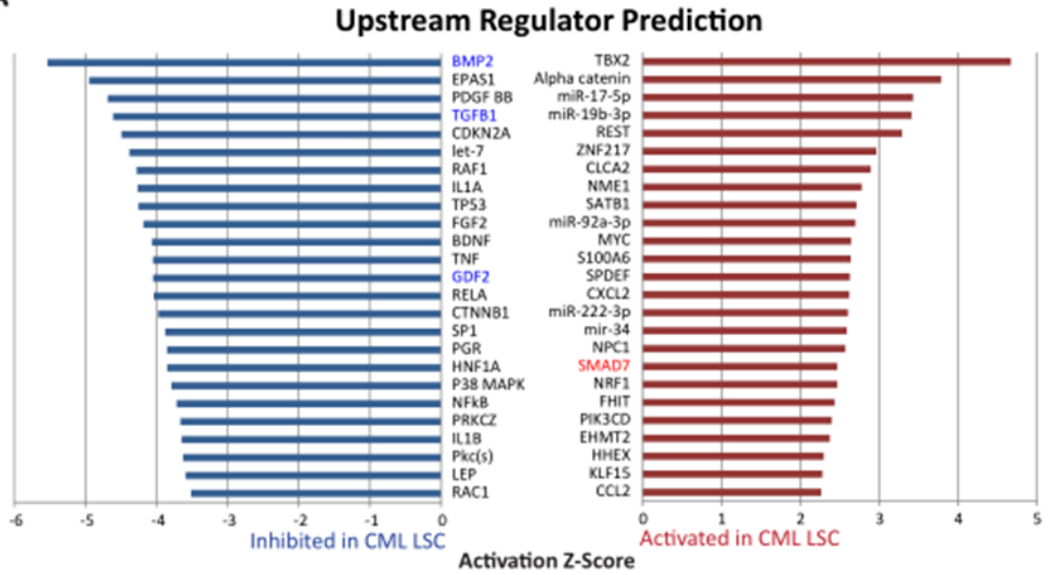


Figure 2.3. Altered cellular functions and pathways in CML LSCs compared to normal HSCs. Gene-set enrichment analyses (GSEA) were carried out to identify upregulated or downregulated GO and KEGG terms in CML versus normal CD34⁺CD38⁻ALDH^{high} cells. Upregulated or downregulated GO and KEGG terms were categorized by common cellular function among a group of associated terms, indicated by bar color. Gene sets with a q-value < 0.01 (red dotted line) were considered significant. Q-value represents the false discovery rate of the p-value, as previously described.⁷² Top three GO or KEGG terms in each category are shown. **Bold** text indicates KEGG terms. *Italicized* text indicates GO terms.

Figure 2.4

A



B

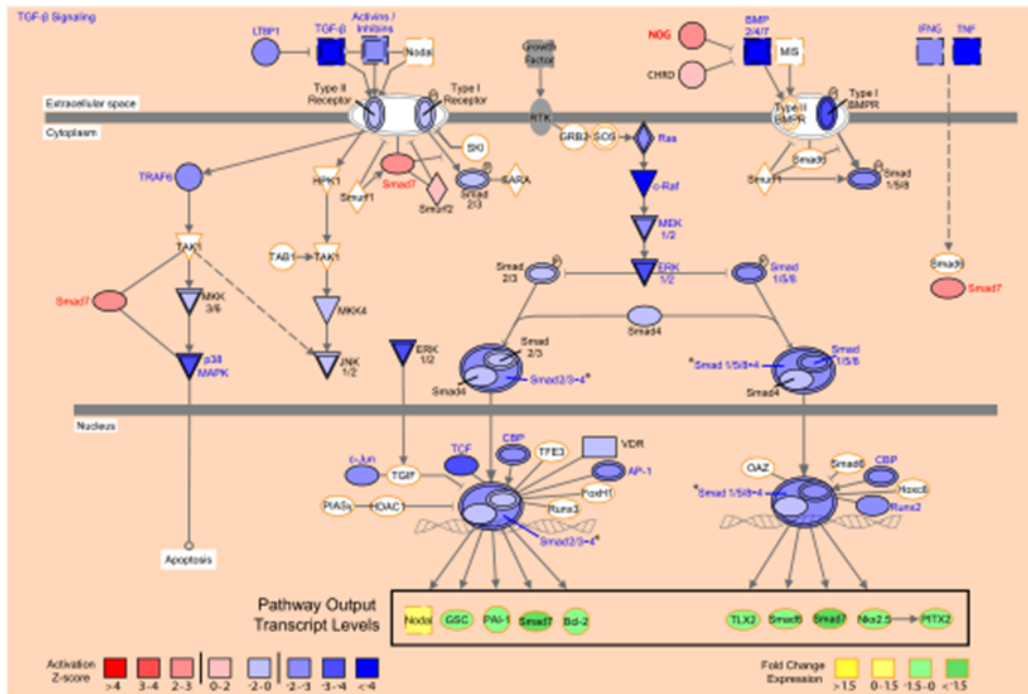


Figure 2.4. TGF-beta signaling pathway activity is altered in CML LSCs. A) The IPA Upstream Regulator analysis was used to identify key regulatory molecules predicted to explain the gene expression differences observed between CML and normal CD34⁺CD38⁻ALDH^{high} cells. Activation Z-scores were calculated for each candidate regulator. Upstream regulators with Z-scores > 2 were considered to be activated (red bars) in CML CD34⁺CD38⁻ALDH^{high} cells. Those with Z-scores < -2 were considered to be inhibited (blue bars) in CML CD34⁺CD38⁻ALDH^{high} cells. Names of activated or inhibited TGF-β pathway members are distinguished in red or blue text, respectively. B) TGF-β signaling pathway. Activated upstream regulators are colored in red; inhibited, blue. Red to blue gradient denotes Z-score value. Activated molecules with a significant Z-score > 2 are distinguished with red text; Inhibited molecules with a significant Z-score < -2, blue text; upstream regulators with a Z-score between -2 and 2, black text. White molecules with orange outline are not considered upstream regulators by IPA. Shape of molecule corresponds to molecule type, as described (Ingenuity® Systems, www.ingenuity.com). A group of molecules with similar functions, depicted by a slash (/) in group name, is colored by a representative molecule with the greatest absolute value Z-score. *indicates a complex of upstream regulators where the activity of the complex is dependent on the activity of all molecules represented. In this case, a separate Z-score was assigned for the complex as a whole and is colored accordingly. Fold change expression values of pathway output transcripts are colored by yellow to green gradient. Yellow indicates upregulation and green, downregulation, of gene expression observed by differential expression analysis of microarray, as discussed in “Methods”.

Figure 2.5

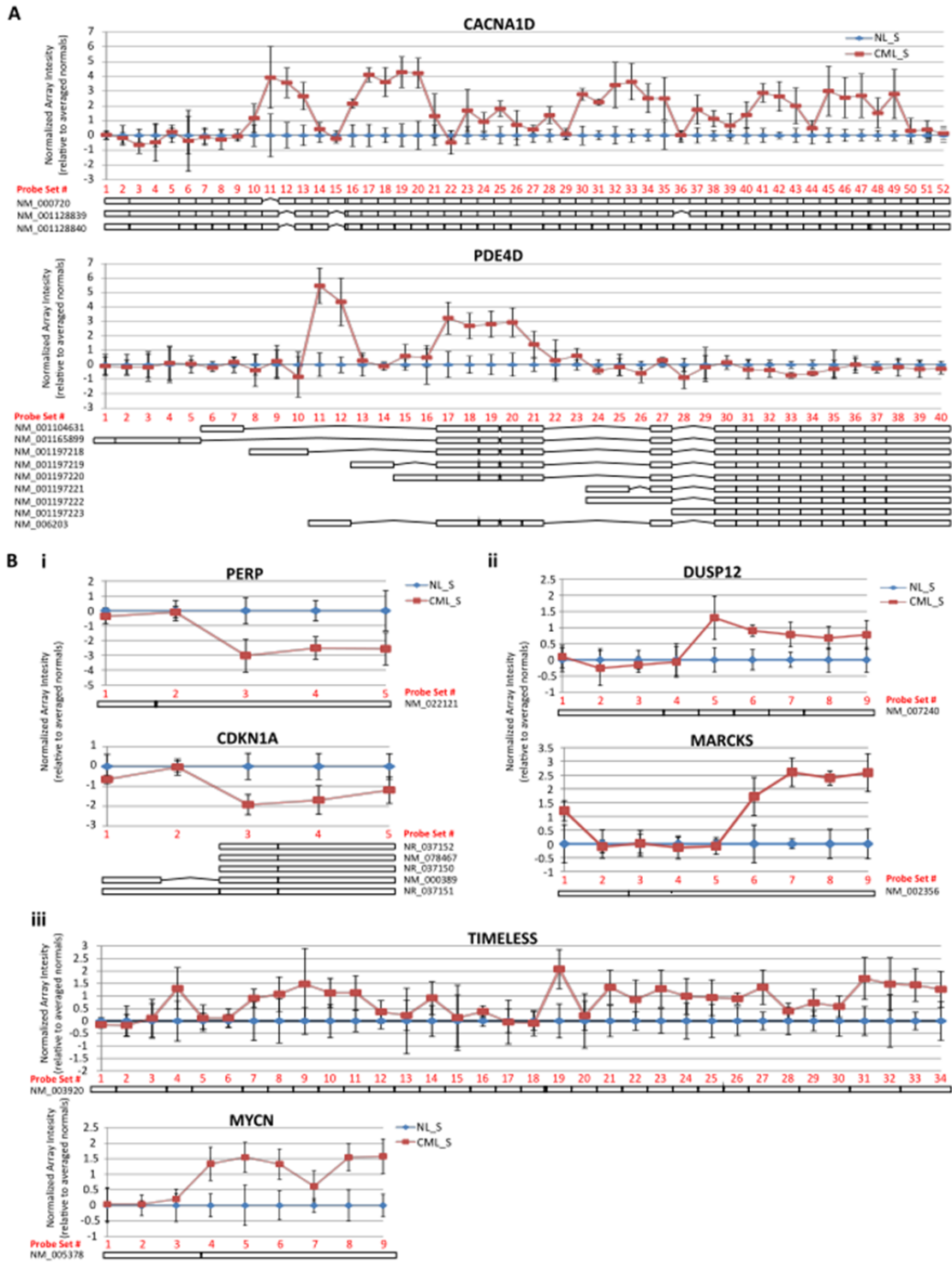


Figure 2.5. Exon-level analysis reveals evidence of alternative splicing in CML

LSCs. A) Exon-level microarray data was analyzed for evidence of alternative transcript expression by ANOVA using the default conditions on the Partek alternative transcript workflow. Genes with an alternative splicing p-value < 0.01 were considered significant. The top two genes with the most significant alternative splicing p-values are shown. For each probeset within a gene, the $\log_2(\text{normalized intensities})$ for each sample was adjusted by the average normalized intensity of the normal samples. The resulting mean and standard deviation for CML or normal samples was plotted according to probeset number, assigned 5'-3', for each representative gene. B) Functional annotation of genes with a p(alternative splicing) < 0.01 revealed that alternative transcripts in CML compared to normal $\text{CD34}^+\text{CD38}^-\text{ALDH}^{\text{high}}$ cells were enriched for genes involved in pathways commonly altered in cancer; (i) p53 signaling, (ii) kinase binding, (iii) cell proliferation. Plots were constructed based on the human reference genome hg19 (GRCh37). Schematics of known refseq transcriptional isoforms are positioned below each graph and are drawn with respect to location of probesets interrogating each exon/intron.

**CHAPTER 3: THE EPIGENETIC REGULATOR UHRF1 IN NORMAL
HEMATOPOIESIS**

Introduction

Hematopoiesis is a complex and tightly regulated process integrating both genetic and epigenetic mechanisms for the maintenance of homeostasis. Dysregulation of these processes can perturb the delicate balance between HSC self-renewal and differentiation programs and result in pathologies related to under- or over-production of HSCs, as in bone marrow failure syndromes or hematologic malignancies. The clinical success of DNA methyltransferase inhibitors in myelodysplastic syndromes and acute leukemias²⁰ establishes the importance of epigenetic regulatory mechanisms in HSC function. Likely contributing to the efficacy of these agents, DNA methylation modifying genes, *TET2*, *IDH1/2*, and *DNMT3A*, were found to be frequently mutated in AML^{73,74}. In addition, components of epigenetic machinery have been nominated as promising therapeutic targets⁷⁵, further underpinning the critical role of epigenetic pathways in HSC maintenance.

The use of genome-wide DNA methylation profiling techniques in both mouse and human have begun to elucidate possible genes and pathways involved in lineage commitment^{15,17}. These studies have largely focused on DNA methylation patterns and were limited to more downstream commitments by hematopoietic progenitors or heterogeneous bulk CD34+ populations. *DNMT1* deficient mice were found to have reduced HSC self-renewal and impaired lymphoid differentiation^{16,76}, establishing a critical role for DNA methylating enzymes in HSC maintenance. Recent studies investigating the mechanism of DNA methylation maintenance have identified UHRF1 as an essential cofactor required for DNMT1 activity. UHRF1 recognizes hemimethylated DNA and recruits DNMT1 to the replication fork^{77,78}. Through its multiple functional

domains, UHRF1 has been shown to recruit HDAC1⁷⁹, bind di- and tri-methyl H3K9⁸⁰, and confer E3 ubiquitin ligase activity on histone H3⁸¹, linking DNA methylation with histone modes of epigenetic regulation⁸². UHRF1 has been shown to be overexpressed in many cancers, including leukemias⁸³, and functions in the silencing of tumor suppressor genes via promoter hypermethylation⁷⁹ as well as ubiquitination-mediated degradation⁸⁴. These observations suggest that *UHRF1* promotes tumorigenesis and is, therefore, a potential therapeutic target⁸⁵. Despite its critical role in DNA methylation maintenance and more recent implications in tumorigenesis, the functional importance of *UHRF1* in the reading and inheritance of epigenetic marks that dictate normal tissue development has largely been understudied.

Utilizing hematopoiesis as a paradigm of epigenetic regulation of stem cell fate decisions and tissue-specific differentiation programs, we employed genome-wide gene expression analysis to identify critical epigenetic regulatory factors that contribute to the phenotypic changes observed in the hematopoietic stem to progenitor cell transition. Furthermore, we show that *UHRF1* is an essential factor in maintenance of adult hematopoiesis in a mouse model.

Methods

Patient samples and microarray analysis

Bone marrow specimens from five healthy donors were enriched for stem and progenitor cell fractions, and gene expression changes were analyzed using whole transcriptome exon microarrays, as previously described⁸⁶. Array intensities from paired stem (CD34⁺ CD38⁻ ALDH^{high}) and progenitor (CD34⁺ CD38⁺) samples were normalized to each other, and one-way paired ANOVA of gene expression summaries was used to identify

differentially expressed genes. Genes with $|\log_2(\text{fold-change})| > 1$ and false discovery rate (FDR) of 0.05 were identified as significantly differentially expressed. This list of genes was searched manually for overlap with known genes involved in epigenetic pathways, including histone or DNA modifying proteins, chromatin remodeling factors, histone chaperones, or essential cofactors in modifying complexes⁸⁷. Hierarchical clustering of Z-score transformed array intensities matching the overlapping gene list was performed according to default conditions(<https://software.broadinstitute.org/morpheus/>).

Mice

All procedures were approved by the Institutional Animal Care and Use Committee at the Johns Hopkins University School of Medicine. Mice heterozygous for a “knockout first” allele targeting exon 3 of UHRF1 were purchased from the European Mutant Mouse Archive (EMMA) as strain B6Dnk;B6N-Uhrf1^{tma1(EUCOMM)Wtsi/leg}. These mice were crossed to FLPe mice (Jackson Laboratories) to remove the gene trap and generate mice with conditional potential through loxp sites flanking exon 3 (*Uhrf1*^{fl/fl}). B6.Cg-Tg(Mx1-cre)1Cgn/J (referred to as Mx1-Cre) mice were obtained as a gift from the laboratory of Gabriel Ghiaur and were crossed to *Uhrf1*^{fl/fl} to generate *Mx1-Cre;Uhrf1*^{wt/fl}. *Mx1-Cre*⁺ and *Mx1-Cre*⁻; *Uhrf1*^{wt/fl} littermates were crossed to produce all genotypes used in experiments: *Uhrf1*^{wt/wt}, *Uhrf1*^{wt/fl}, *Uhrf1*^{fl/fl} and *Mx1-Cre;Uhrf1*^{wt/wt}, *Mx1-Cre;Uhrf1*^{wt/fl}, *Mx1-Cre;Uhrf1*^{fl/fl}. All mice used for experiments were 8-12 week old littermates. PIPC (Invivogen) was injected intraperitoneally every other day at 250ug for 4 or 5 total injections. Total injection number (4 or 5 injections) was not associated with statistically significant differences in mouse phenotypes, independent of genotype. All figures represent mice that received 4 total injections, unless otherwise noted. *Uhrf1*^{wt/Δ} and

Uhrf1^{Δ/Δ} symbols describe the genotypes of mice in which PIPC injections were given to induce Cre expression, resulting in the recombination of loxP sites and deletion of *Uhrf1* loci. Phenotypic analysis of all injected mice was performed at 19 days after the first PIPC injection, unless otherwise specified.

Tissue Collection and Histology

Peripheral blood was collected by submandibular venous puncture into a heparin-coated capillary tube and transferred to a K3EDTA vial. Differential counts were obtained on a ProCyte Dx A5904 (Idexx Laboratories, Inc.) in the JHU mouse phenotyping core facility. At specified timepoints, mice were euthanized by CO₂ and cervical dislocation. Spleen, kidney, liver, and tail specimens were harvested, flash-frozen in liquid nitrogen, and stored at -80 C. Bone marrow was extracted from femurs, tibiae, iliac crests, and spine of each mouse by crushing with a mortar and pestle, as previously described⁸⁸. One million bone marrow cells or 50uL of blood were reserved and flash-frozen for DNA analysis. Fresh bone marrow or blood was used for complete blood counts and flow cytometric analysis. Humeri from PIPC injected mice were fixed for 48 hours in phosphate-buffered formalin, then stored in PBS at 4 C until further processing. Fixed bones were submitted to the JHU Oncology Tissue Services core facility for decalcification, paraffin block preparation, and hematoxylin and eosin staining (H&E). Images of stained bone sections were taken at 400x magnification.

DNA extraction and genotyping

Genomic DNA was extracted from frozen tissue using a DNeasy Blood and Tissue kit (Qiagen) according to manufacturer's instructions. Genotyping PCR was performed by amplifying 30ng of genomic DNA with the following primers (5'-3'):

LoxP_F: CTTGATCTGTGCCCTGCAT

LoxP_R: ACCTCTGCTCTGATGGCTGT

UHRF1,del_R: CCGAGGACACTCAAGAGAGC.

PCR reactions underwent electrophoresis on a 2% agarose gel, and band intensities were quantified using GeneTools imaging software (Syngene).

Flow cytometry

Mouse blood or bone marrow samples were treated according to manufacturer's instructions with RBC lysis buffer (ebioscience) to eliminate red cell contamination during flow cytometric acquisition. Following lysis, blood samples were labeled with fluorochrome-conjugated antibodies. For bone marrow analysis, stem and progenitor populations were identified using biotin-labeled CD3 (145-2C11), B220 (RA3-6B2), Gr1 (RB6-8C5), and Ter119, PerCP-Cy5.5-streptavidin, Pe-Cy7-Sca1 (D7), APC-cKit (2B8), PE-Flt3 (A2F10.1) acquired from BD Pharmingen, and APC-eFluor®780-IL7Ra (A7R34) from eBioscience. For the UHRF1 flow cytometric assay, cells were fixed and permeabilized using a Foxp3 intracellular staining kit according to manufacturer's instructions (eBioscience). UHRF1 antibody was obtained from LSBio (Th-10a) and conjugated to Ax647 via an antibody labeling kit (Molecular Probes).

Blood and bone marrow specimens from congenic mice were distinguished by FITC-CD45.1 (A20) and PE-CD45.2 (104) antibodies, and lineage repopulation was

determined using PerCP-Cy5.5-B220, Pe-Cy7-CD3, APC-Mac1 (M1/70), and APC-Gr1 (BD Pharmingen). For each experiment, viable bone marrow cells were distinguished using Fixable Viability Dye eFluor® 450 (ebioscience), whether cells ultimately underwent fixation or not. All samples were acquired on a LSRII flow cytometer (BD Biosciences), and data were analyzed using FlowJo software version 10.2 (Treestar).

Transplantation assays

Congenic CD45.1+ recipient mice (B6.SJL-Ptprca Pepcb/BoyJ, Jackson Laboratories) were lethally irradiated with a split dose (8+4 Gy) delivered less than 4 hours apart. WT competitor cells were obtained from the F1 cross of WT CD45.1 (Jackson laboratories) and WT CD45.2 mice (*Uhrf1^{wt/wt}*, without *Mx1-Cre*). All mice used in experiments were 8-12 weeks old. To generate chimeric transplanted mice, 1×10^6 unfractionated CD45.2 donor WBM mixed with 1×10^6 WT CD45.1/CD45.2 competitor WBM was transplanted by tail-vein injection into lethally irradiated CD45.1 female recipient mice. Peripheral blood engraftment was assessed at 11 weeks post-transplant. PIPC was delivered intraperitoneally at 250ug for 4 total injections. Peripheral blood chimerism was assessed for 24 weeks following the first injection. At week 25, recipient mice were euthanized, and tissues were harvested for further analysis.

Statistics

All statistical analyses used in mouse studies were performed using GraphPad Prism version 5.01 (GraphPad Software, San Diego California USA, www.graphpad.com). P-values were calculated by unpaired t-test, unless otherwise noted.

Results

Identification of UHRF1 as a critical epigenetic regulatory factor in hematopoietic development

In order to investigate the regulatory mechanisms involved in normal hematopoietic development, we analyzed whole transcriptome gene-level expression data from highly enriched stem ($CD34^+CD38^-ALDH^{high}$) and progenitor ($CD34^+CD38^+$) fractions obtained from five healthy bone marrow donors⁸⁶. ANOVA was used to nominate differentially expressed genes that may define critical mediators involved in the regulation of normal hematopoietic stem to progenitor cell transition. A total of 1183 transcripts were found to be significantly differentially expressed in $CD34^+CD38^-ALDH^{high}$ compared to $CD34^+CD38^+$ populations (FDR = 0.05, $|\log_2(\text{Fold Change})| > 1$). Of these, 45 transcripts were identified as known factors involved in epigenetic regulatory mechanisms⁸⁷ (Figure 3.1). These include *EZH2* (FC -3.94, $p = 5.57E-6$), *DNMT1* (FC -3.03, $p = 8.66E-6$), and *TET2* (FC 2.07, $p = 3.13E-4$), which have been implicated previously in normal or malignant hematopoietic development, along with *UHRF1* (FC -3.73, $p = 8.10E-5$), a known DNMT1 binding partner. These expression data, combined with the known multifunctional role of *UHRF1* in reading both histone tail and DNA modifications, suggest *UHRF1* is an important epigenetic regulator of differentiation programs in hematopoiesis.

Generating an inducible, conditional UHRF1 knockout mouse model

In adult mice, hematopoietic stem and progenitor cell subtypes are easily identified by well-defined cell surface markers², making the mouse an ideal model to study HSC differentiation. Previous studies have shown constitutive, homozygous

deletion of *Uhrfl* in a conventional knockout mouse model results in embryonic lethality by E9.5⁷⁸. Attempts to breed a conditional knockout, specific to the hematopoietic system via a *Vav1-Cre* model, failed to yield viable *Uhrfl*^{Δ/Δ} pups (data not shown). In order to assess the role of *Uhrfl* specifically in adult hematopoiesis, we sought to generate an inducible, conditional knockout mouse. Mice with *loxP* sites flanking exon 3 of *Uhrfl* (*Uhrfl*^{fl/fl}) were crossed to *Mx1-Cre* transgenic mice, and deletion was induced by intraperitoneal injection of PIPC in 8-12 week old adults (Figure 3.2A). Homozygous *Uhrfl* deletion efficiency was assessed by genomic PCR of whole bone marrow (WBM) 19 days after initial injection (mean ± SD: 75.4±10.4%, n=10) (Figure 3.2B). Coordinate depletion of protein expression was measured by flow cytometry in *Uhrfl*^{Δ/Δ} WBM, while expression levels were maintained in *Uhrfl*^{wt/Δ} compared to *Mx1-Cre;Uhrfl*^{wt/wt} control mice (Figure 3.2E,F). Because Cre expression is controlled under the *Mx1* promoter in this model, all cells that produce an IFN response will induce *Uhrfl* deletion. Due to this, we assessed homozygous deletion by genomic PCR in non-hematopoietic tissues as well as the spleen, the major site of extramedullary hematopoiesis. Although efficiency of homozygous deletion in the spleen was comparable to that in bone marrow specimens (Figure 3.2C), spleen weight was not significantly affected. In heterozygous knockout mice, the significant increase compared to controls was not determined to be physiologically relevant upon consideration of the range of spleen weights in PIPC-injected *Uhrfl*^{fl/fl} mice. Therefore, we chose to focus subsequent analyses on the effects of *Uhrfl* depletion in hematopoietic development in the bone marrow.

Homozygous deletion of UHRF1 in adult hematopoiesis

Homozygous deletion of *Uhrfl* induced rapid lethality in all mice by 21 days post-injection (Figure 3.3A; median survival 18 days, n=6, p < 0.001). Genomic deletion was confirmed in moribund WBM specimens (Figure 3.3B). At 19 days after PIPC injection, peripheral blood counts revealed pancytopenia, as seen in all mature lineages of the blood (Figure 3.3C). Massive bone marrow hypoplasia was apparent in histological sections of humerus and confirmed by absolute cell counts of viable WBM (Figure 3.3D,E). Notably, this extreme phenotype was not seen in the bone marrow of heterozygous knockout mice. Although blood counts from the erythroid lineage of *Uhrfl^{wt/Δ}* mice reached statistical significance compared to controls, the mild reduction in counts did not reach physiological significance, as the counts did not qualify as anemic or affect overall survival. Further analysis of bone marrow stem and progenitor populations revealed significantly reduced frequencies of Kit-expressing cells, including bulk stem cell (LSK, Lin-Sca+Kit+) and myeloid progenitor (MP, Lin-Sca-Kit+) populations, with a complete absence of a common lymphoid progenitor (CLP, Lin-Flt3+IL7Ra+) population, in *Uhrfl^{Δ/Δ}* compared to *Uhrfl^{wt/Δ}* and control mice (Figure 3.4A,B).

Competitive Bone Marrow transplantation

Due to the hierarchical nature of hematopoietic development and the complex feedback mechanisms regulating its homeostasis, absence of a committed or terminally differentiated population activates proliferation and differentiation programs in stem and progenitor populations to replenish low cell numbers in more mature populations⁸⁹. One possible scenario to explain the global reduction in all bone marrow and blood cell populations in *Uhrfl^{Δ/Δ}* mice is a requirement of UHRF1 expression for survival in one or

more lineage committed cell populations but not in the stem and progenitor cell compartments. A cycle of cell death in mature populations followed by proliferation of immature cells would eventually lead to exhaustion of stem and progenitor compartments, independent of an autonomous requirement of UHRF1.

In order to distinguish a role for *Uhrfl* in each individual subpopulation along the hematopoietic hierarchy, we introduced WT cells in a competitive transplantation model to reduce the burden of daily hematopoietic requirements on *Uhrfl* knockout cells and eliminate the limitations of the rapid lethality phenotype. To generate chimeric mice harboring both *Uhrfl*^{Δ/Δ} and WT hematopoiesis, lethally-irradiated recipient mice were injected with whole bone marrow (WBM) from either *Mx1-Cre;Uhrfl*^{fl/fl} or *Mx1-Cre;Uhrfl*^{wt/wt} control mice that was mixed 1:1 with WT competitor marrow. Whole bone marrow from WT mice lacking the *Mx1-Cre* transgene was used as an additional donor control to account for any deleterious effects of Cre expression. Donor (CD45.2), competitor (CD45.1/CD45.2), and host (CD45.1) mice were bred on congenic CD45 backgrounds in order to trace the origin of engrafted bone marrow populations. Peripheral blood engraftment was confirmed at 11 weeks post-transplantation, and all mice were injected with PIPC (Figure 3.5A). Long-term follow-up showed a significant and steady decline in peripheral blood engraftment of *Uhrfl*^{Δ/Δ} donor marrow after PIPC injection (Figure 3.5B). Assessment of multi-lineage repopulation beyond 16 weeks did not show any stable, statistically significant changes in donor contribution to myeloid (Mac1+ and/or Gr1+), B cell (B220+), or T cell (CD3+) lineages compared to controls (Figure 3.5C). Genotyping of peripheral blood at 16 weeks post-injection confirmed the presence of homozygous deleted cells in the remaining terminally differentiated donor

populations (Figure 3.5D), suggesting that these mature blood cells were generated from a *Uhrf1*^{Δ/Δ} long-term repopulating subpopulation in the bone marrow. Together, these data indicate that a long-term primitive cell that is void of UHRF1 expression is capable of producing all mature populations in the blood but at a greatly reduced efficiency compared to WT competitor cells.

In order to determine the potential source of *Uhrf1*^{Δ/Δ} cells in the periphery, CD45.2⁺ donor marrow was examined for the presence of stem and progenitor populations and revealed a near absence of LSK, MP, and CLP fractions (Figure 3.6A,B). Although the CLP (Lin- Flt3⁺ IL7Ra⁺) population was absent in bone marrow from *Uhrf1*^{Δ/Δ} donors, the bulk Lin- IL7Ra⁺ population was overrepresented in total marrow compared to control donors (Figure 3.6C, left panel), with IL7Ra⁺ cells comprising over half of the Lin- compartment (Figure 3.6C, right panel). Since Flt3 has been shown to be essential during early stages of B-lymphopoiesis⁹⁰, the presence of a Lin- Flt3- IL7Ra⁺ population suggests that a potential lymphoid-committed cell that is more differentiated than the CLP remains in *Uhrf1*^{Δ/Δ} marrow. To investigate this further, we gated on CD45.2⁺ donor cells to assess the contribution of *Uhrf1*^{Δ/Δ} cells to mature populations in the bone marrow. We exploited the differences in side scatter distribution and CD45 expression to distinguish bulk lymphoblast, granulocyte, and lymphocyte populations. We first confirmed the loss of UHRF1 expression in *Uhrf1*^{Δ/Δ} donor cells to ensure that any residual hematopoiesis was not due to remaining cells with floxed alleles that failed to recombine upon PIPC injection (Figure 3.6D,E). In viable WBM of control mice, all three major bulk populations are represented. In contrast, lymphocytes are overrepresented in knockout donor marrow, with near absent blast and granulocyte

populations (Figure 3.6D,F). After gating on UHRF1+ cells from control donor marrow, only granulocytes and blasts remain, while lymphocytes are nearly absent (Figure 3.6D,F). These data indicate that a majority of mature lymphocytes do not express UHRF1 and suggest that a loss of dependence on UHRF1 expression for survival and differentiation occurs within a Lin- IL7Ra+ progenitor subset that is capable of maintaining a mature lymphocyte population.

Discussion

Understanding the epigenetic regulation of transcriptional programs responsible for guarding HSC function is of great interest due to the broad clinical applications of HSC transplantation and the contribution of aberrant pathway regulation to malignant transformation. In this study, we have identified several important factors involved in epigenetic regulatory mechanisms and demonstrate that UHRF1 is essential for hematopoietic stem and progenitor function and lineage commitment programs.

Genome-wide gene expression analysis of highly-refined stem and progenitor fractions from healthy bone marrow donors revealed that key epigenetic regulatory factors, including *DNMT1*, *EZH2*, *TET2*, and *UHRF1* were differentially expressed in the early commitment decisions of hematopoietic stem cells. These findings were consistent with recent studies in knockout mice and indicate a role for DNA methylation and histone modifying proteins in hematopoietic development, including the maintenance of self-renewal and lineage commitment decisions of HSCs. *Dnmt1* hypomorphs showed impaired HSC self-renewal and displayed myeloerythroid lineage restriction¹⁶. *Ezh2* knock-in mice demonstrate increased HSC cell number and proliferation with progression to myeloproliferative disorder⁹¹. Similarly, studies using *Tet2*-deficient mice showed

increased HSC self-renewal and myeloproliferation in vivo, with progression to a transformed phenotype⁹². Furthermore, *EZH2* and *TET2* have also been shown to be mutated in hematologic malignancies, validating the essential role for chromatin-modulating proteins in the stable inheritance of HSC functional programs^{73,93}.

Because the role of UHRF1 in hematopoiesis was not previously explored, we next studied the role of UHRF1 in murine hematopoiesis. Homozygous deletion of UHRF1 in adult hematopoiesis induced rapid lethality in all mice with profound blood and bone marrow deficiencies, similar to the phenotypes observed in an Mx1-cre DNMT1 knockout mouse model¹⁶. This is consistent with the function of UHRF1 in DNA methylation maintenance. This profound phenotype contrasted with results from Trowbridge et al.⁷⁶, but differences may have been due to differing PIPC injection doses and schedules resulting in incomplete DNMT1 knockout in that prior study. When hematopoiesis was supported with the addition of WT competitor cells in a transplantation model, we were able to circumvent the limitations of the rapid lethality phenotype and isolate specific cell lineages that were most affected by loss of UHRF1 expression. These data confirmed the complete ablation of primitive cell compartments seen in initial experiments but, surprisingly, B- and T- lymphoid and myeloid mature cells were still detectable in the periphery. Previous results from DNMT1 hypomorphs indicated an essential role for DNA methylation in suppressing myeloid developmental pathways for lymphopoiesis¹⁶. In this study, we propose that UHRF1-dependent epigenetic regulation is critical in early lymphoid development. However, such dependence on UHRF1 may be lost further along lymphoid development, evidenced by an observed lack of Kit-expressing stem and progenitor cells and relative enrichment of

Flt3 negative, IL7Ra-expressing cells within the Lin⁻ compartment of UHRF1 knockout marrow. Supporting this, c-kit-deficient mice showed severely reduced CLP numbers, while prepro- and pro-B cells were not affected⁹⁴. Additionally, a subpopulation of Lin⁻Sca⁺ Kit⁻ (LSK⁻) cells that express high levels of CD25 and are exclusively Flt3-IL7Ra⁺ were able to be generated from CLPs *in vitro*⁹⁵. Although we did not assess CD25 expression in our competitive transplant model, it is possible that the remaining population is heterogeneous and contains lymphoid-primed cells that are more differentiated and lineage restricted than the CLP fraction. Together, this suggests that dependence on UHRF1 may vary during lymphoid development, with complete loss in later stages of lymphopoiesis.

Our observations confirm that genes involved in epigenetic regulatory mechanisms, including factors known to be perturbed in bone marrow disorders, are differentially expressed in hematopoietic stem and progenitor cells from normal bone marrow donors. Also, for the first time, we show that UHRF1 is obligatory for normal HSC function, while its role in lymphoid development may vary with degree of differentiation.

Acknowledgements

I wish to acknowledge Jon Gerber and David Esopi for carrying out cell sorting and RNA preparation procedures for microarray experiments. Thank you to Dave Walker for providing the UHRF1 conditional knockout mice and genotyping primers and to Benjamin Singer for the UHRF1 intracellular stain reagents and protocol. I am especially grateful for Vasan Yegnasubramanian, Gabriel Ghiaur, and Ajay Vaghasia for your expertise and insights into experimental design and data analysis.

Tables and Figures
 Figure 3.1

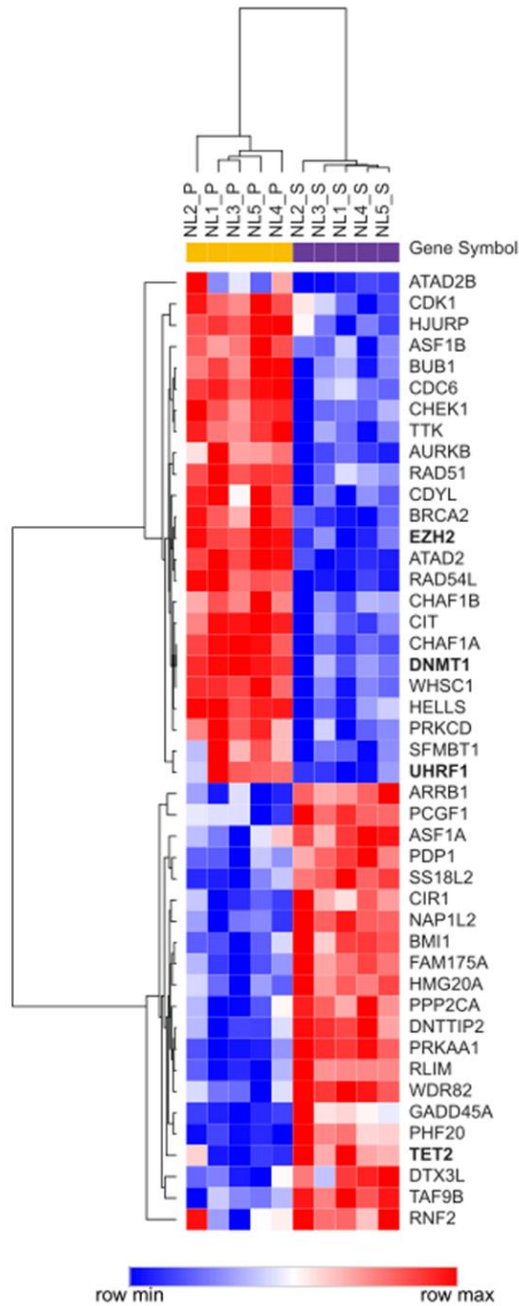


Figure 3.1. Gene expression changes of epigenetic regulatory factors involved in hematopoietic stem to progenitor cell differentiation. Heatmap showing the expression levels of known epigenetic regulatory genes that are differentially expressed between normal stem ($CD34^+CD38^-ALDH^{high}$) and progenitor ($CD34^+CD38^+$) cells with $FDR = 0.05$ and $|\log_2(\text{Fold Change})| > 1$. Upregulated and downregulated expression levels are indicated in red and blue, respectively. Gene symbols in bold represent DNA methylation and Polycomb group factors that have been previously studied in hematopoietic development. NL_S, normal stem cells; NL_P, normal progenitor cells.

Figure 3.2

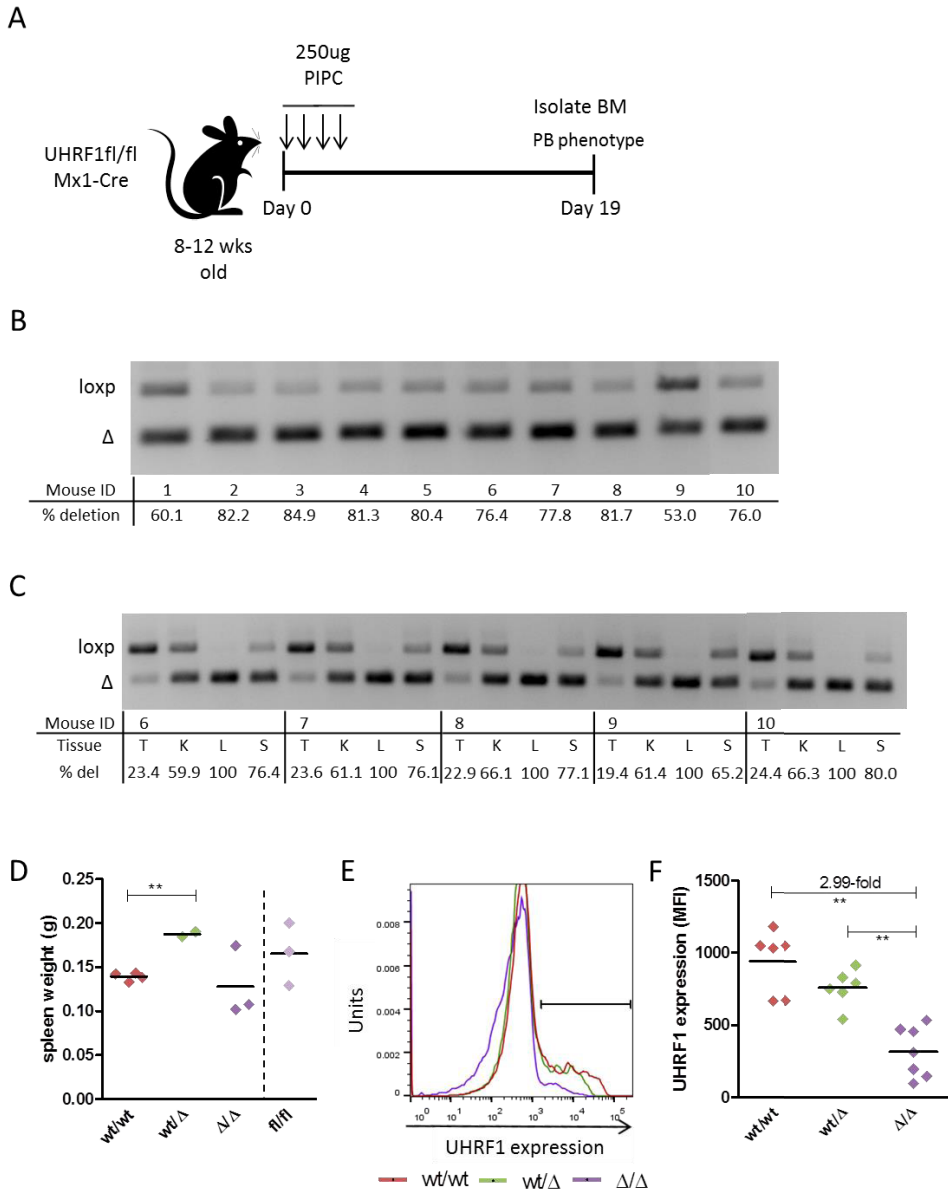


Figure 3.2. Induced conditional deletion of UHRF1 in the hematopoietic system. A) Schematic of mouse model depicting PIPC injection schedule used to induce deletion of *Uhrf1* in the hematopoietic system. All mice received 250ug of PIPC every other day for four total injections. Tissues were harvested 19 days after the first PIPC injection. B,C) Genotyping PCR results of *Uhrf1*^{Δ/Δ} tissues. WBM (B) or tail,T; kidney,K; liver,L; spleen,S (C). D) Dot plot of spleen weights (g) of PIPC injected mice. E,F) UHRF1 expression in viable WBM samples by flow cytometry. Histogram plot of one representative sample of each genotype (E) and dot plot of mean fluorescence intensity, MFI (F). wt/wt (red outline or diamonds) refers to PIPC injected *Mx1-Cre; Uhrf1*^{wt/wt}; wt/Δ (green outline or diamonds), *Uhrf1*^{wt/Δ} (PIP injected *Mx1-Cre; Uhrf1*^{wt/fl}); Δ/Δ (purple outline or diamonds), *Uhrf1*^{Δ/Δ} (PIP injected *Mx1-Cre; Uhrf1*^{fl/fl}). Dot plots: Each point on graph represents one mouse. Black horizontal bars represent means.

Figure 3.3

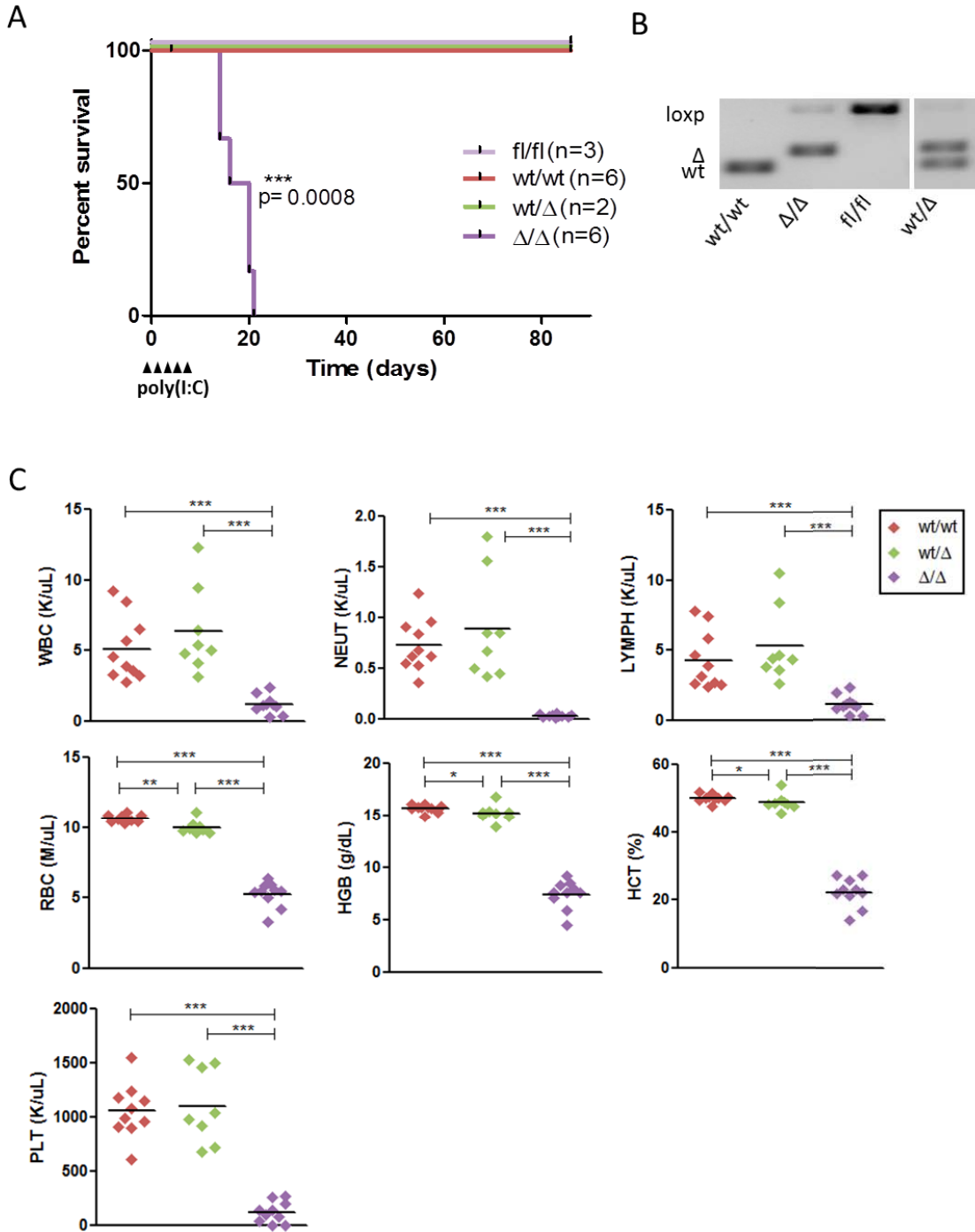
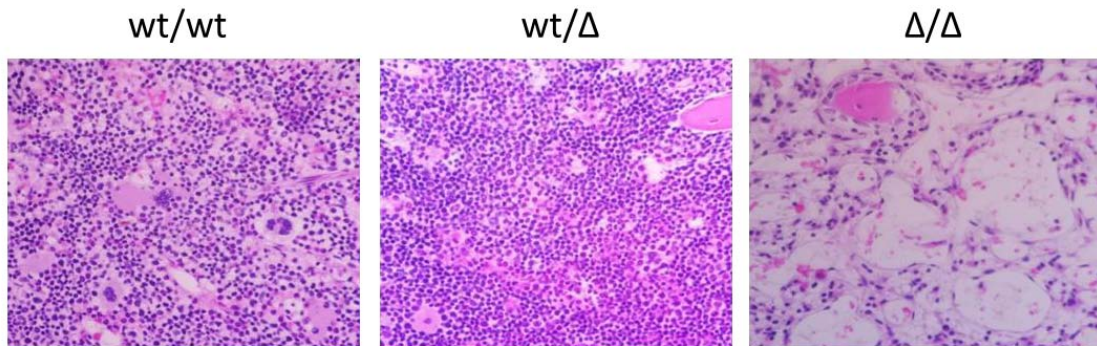


Figure 3.3 (con't)

D



E

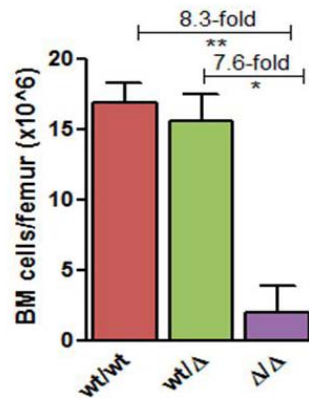


Figure 3.3. Conditional deletion of UHRF1 induces rapid lethality with pancytopenia and diminished bone marrow cellularity. A) Kaplan-Meier curve displaying cumulative survival. Arrow heads represent PIPC injections. $P = 0.0008$ by log-rank test. B) Genotyping PCR results of WBM samples collected at 21 days post-PIPC injection. All genotypes in A,B represent mice that were injected with 250ug PIPC every other day for five total injections. fl/fl, (PIPC injected *Uhrf1^{fl/fl}*, without *Mx1-Cre* transgene). C) Peripheral blood counts at 19 days post-PIPC injection. Horizontal black bar signifies mean. P-values determined by Mann-Whitney test. D) H&E stain of formalin-fixed, paraffin-embedded humerus sections. One representative section per genotype is shown. Original magnification, 400x. E) Absolute bone marrow counts per femur. Viable cells were counted by trypan blue exclusion on a hemacytometer. Bar plots represent mean \pm SD; wt/wt n = 4, wt/Δ n = 2, Δ/Δ n = 3; * $P \leq 0.05$, ** $P \leq 0.01$, *** $P \leq 0.001$.

Figure 3.4

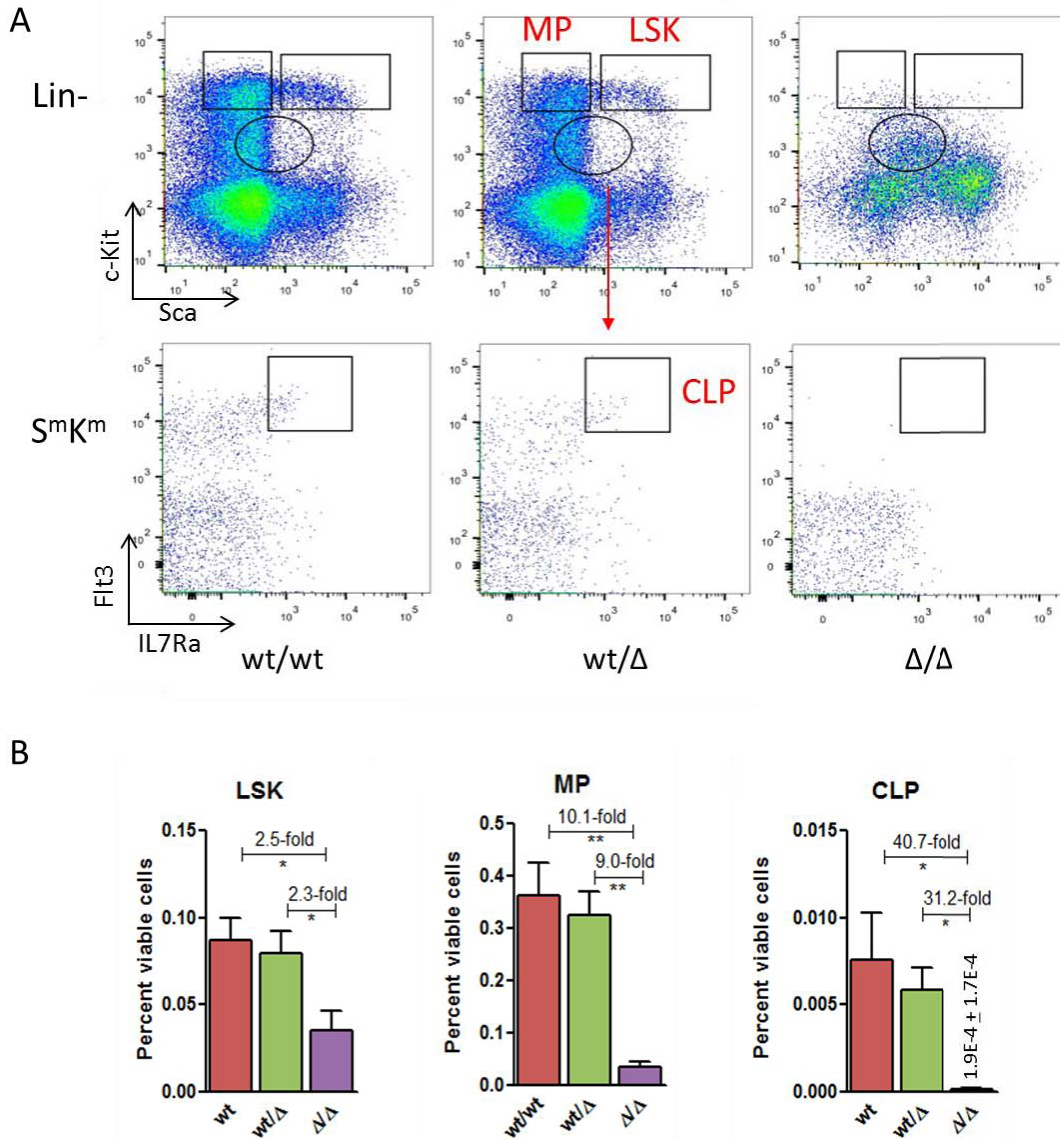
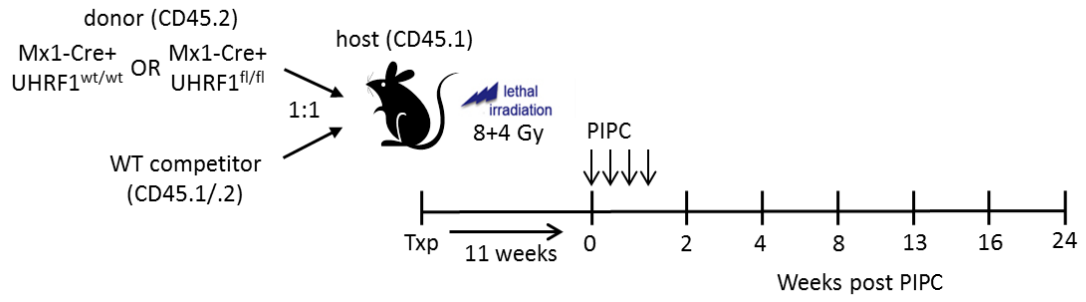


Figure 3.4. Defective HSPC compartment in UHRF1 KO mice. A) Representative FACS plots and gating strategy for bone marrow stem and progenitor populations. Total viable bone marrow was defined by FSC v. SSC size-selection, single cell gating, and viability dye exclusion. Top row: Stem and progenitor fractions of Lin⁻ (CD3⁻, Gr-1⁻, B220⁻, Ter119⁻) bone marrow. Bottom row: CLP fraction of Sca^{mid}Kit^{mid} (S^mK^m) cells. B) Frequency of gated populations in total viable bone marrow. Data expressed as mean \pm SD. *P < 0.05, **P < 0.01. LSK, Lin⁻Sca⁺Kit⁺; MP, myeloid progenitors; CLP, common lymphoid progenitor.

Figure 3.5

A



B

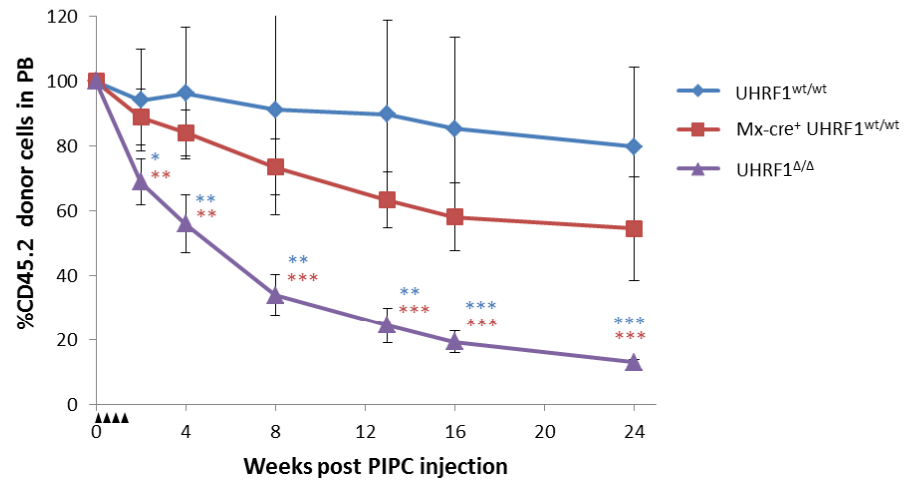
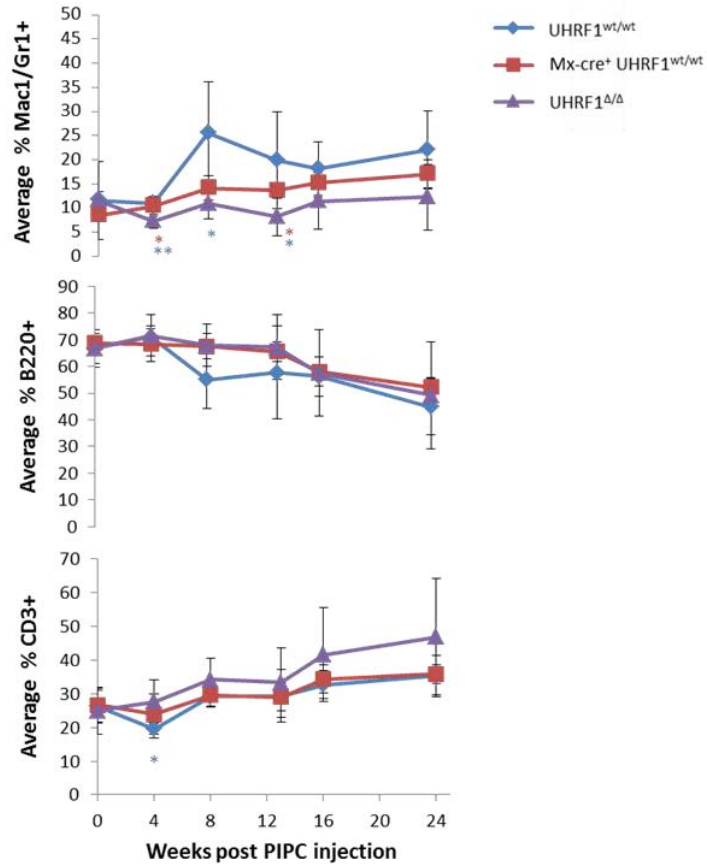


Figure 3.5 (con't)

C



D

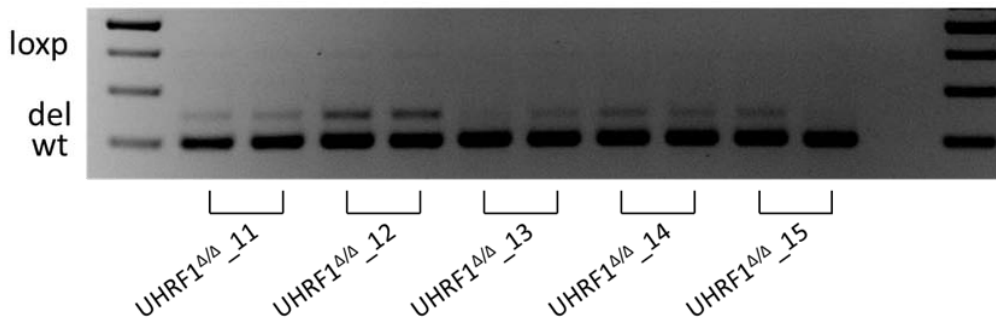


Figure 3.5. Reduced peripheral blood engraftment in UHRF1 KO competitive transplant model. A) Schematic of competitive transplant model. B) Average normalized peripheral blood chimerism of transplant recipients. Arrow heads indicate PIPC injections. C) Average percent Lin⁺ donor cells in peripheral blood. Data in B and C represented as mean \pm SD, n = 5 recipients per genotype at each timepoint. Blue asterisks indicate statistics for UHRF1^{Δ/Δ} vs UHRF1^{wt/wt} donors. Red asterisks indicate UHRF1^{wt/wt} vs Mx1-Cre;UHRF1^{wt/wt} comparison. *P \leq 0.05, **P \leq 0.01, ***P \leq 0.001. D) Genomic PCR results of peripheral blood of recipient mice at 16 weeks post-PIPC injection.

Figure 3.6

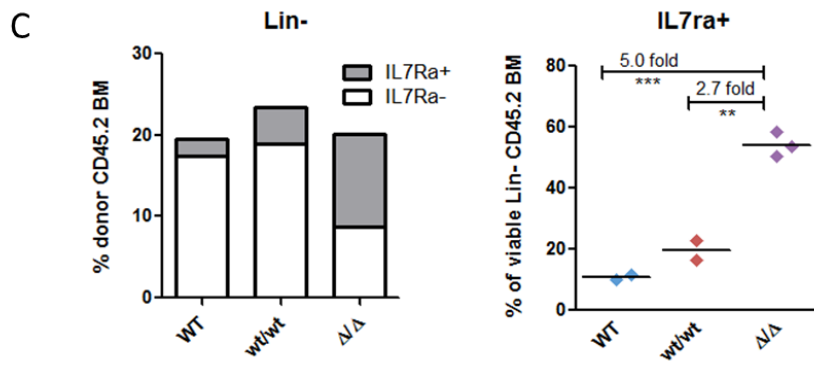
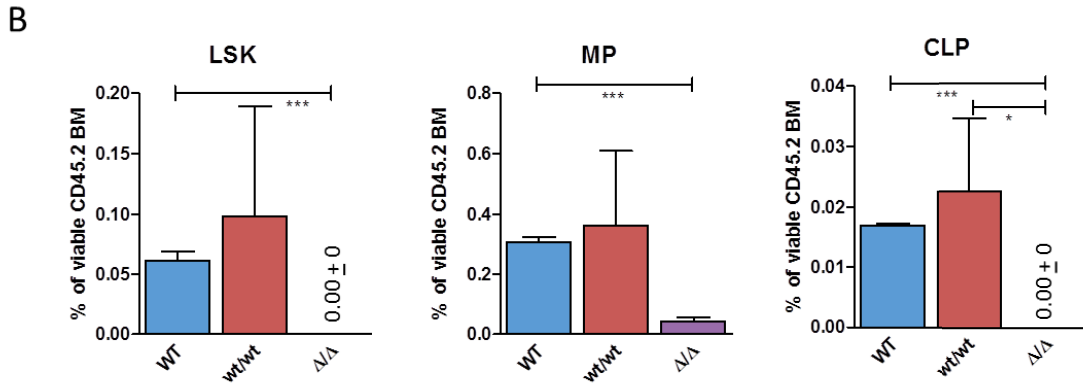
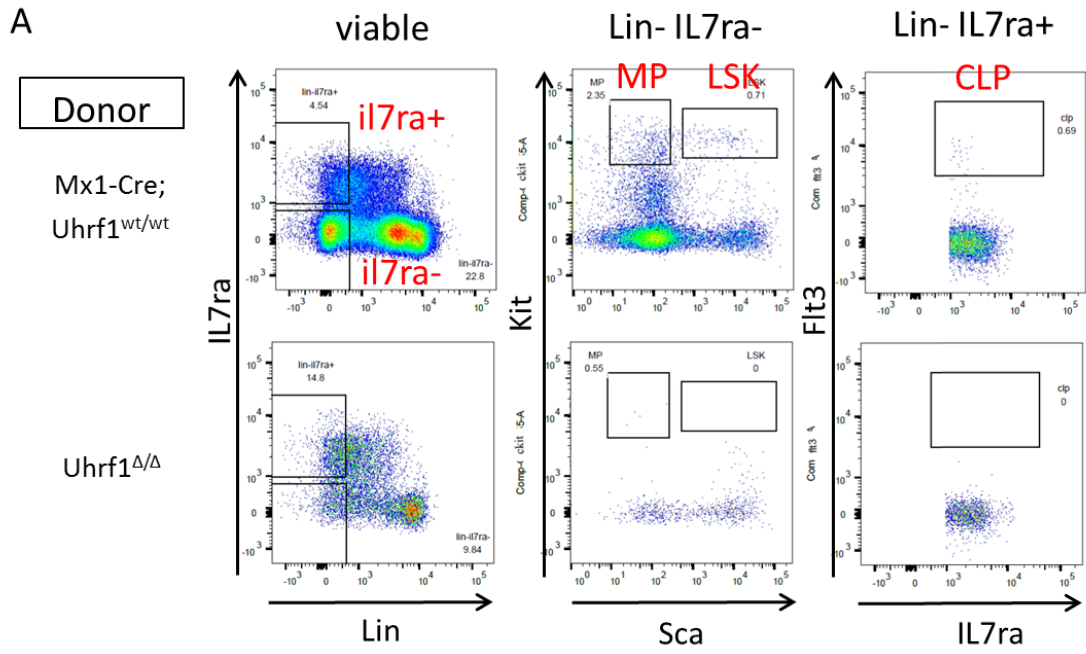
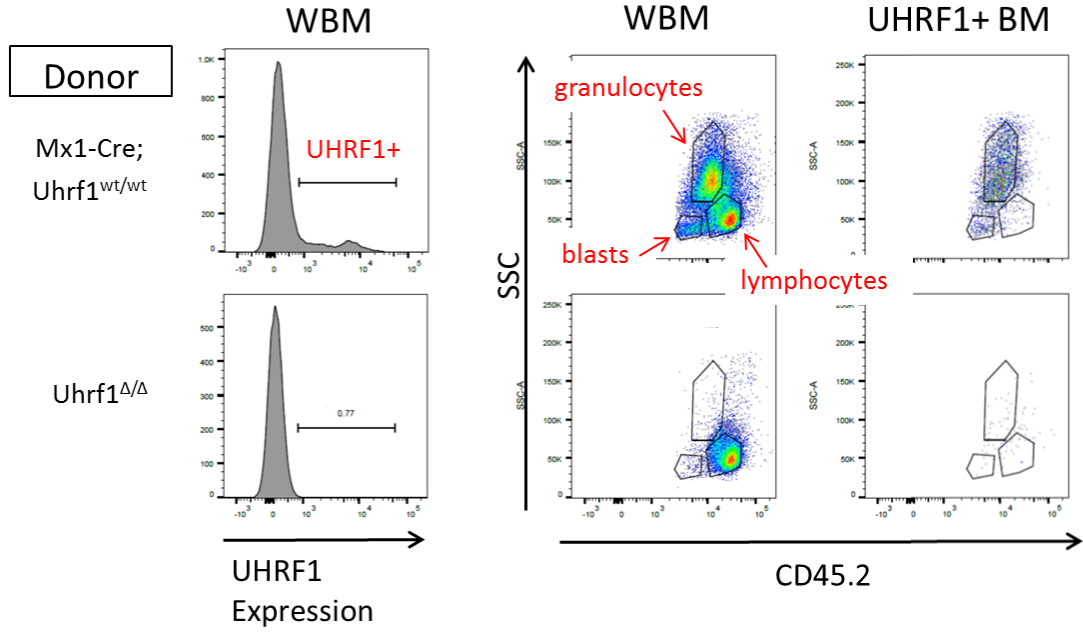
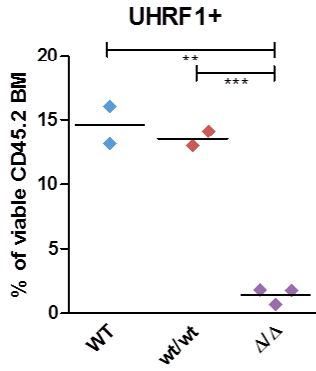


Figure 3.6 (con't)

D



E



F

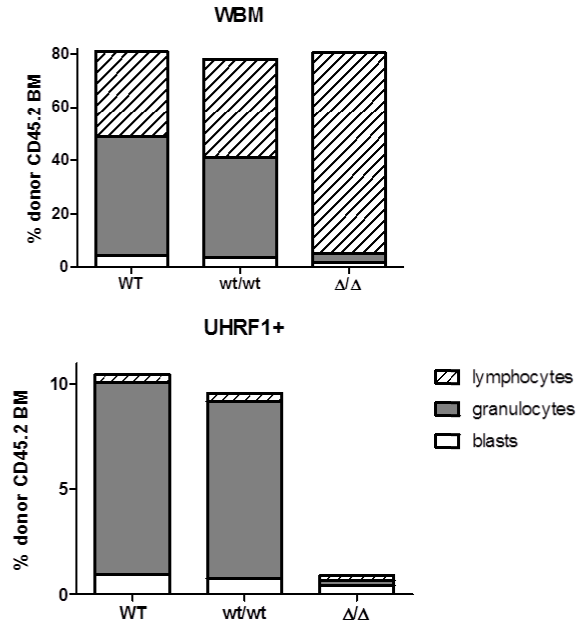


Figure 3.6. Survival of a lymphoid committed population in UHRF1 KO competitive transplant model. A) Representative FACS plots of viable bone marrow from transplant recipient mice at 25 weeks post-PIPC injections. Top row: *Mx1-Cre;Uhrf1^{wt/wt}* viable donor marrow. Bottom row: *Uhrf1^{Δ/Δ}* viable donor marrow. B) Frequency of gated populations represented as percentage of CD45.2 donor marrow for each genotype. Data expressed as mean \pm SD; WT n = 2, wt/wt n = 2, Δ/Δ n = 3; *P < 0.05, **P < 0.01. C) Frequency of IL7Ra+ cells within the Lin- compartment. Left bar plot: Data expressed as mean percentage of total viable CD45.2 donor cells. Right dot plot: Data expressed as percentage of CD45.2 donor Lin- cells. Each point on plot represents one mouse. WT n = 2, wt/wt n = 2, Δ/Δ n = 3; **P < 0.01, ***P < 0.001. D) Representative FACS plots. Top row: *Mx1-Cre;Uhrf1^{wt/wt}* viable donor marrow. Bottom row: *Uhrf1^{Δ/Δ}* viable donor marrow. Histogram plots: UHRF1 expression in total viable bone marrow gated on CD45.2 donor compartment. Dot plots, left column: CD45.2 expression in viable donor marrow. Dot plots, right column: CD45.2 expression in UHRF1+ viable donor marrow. E) Percentage of UHRF1+ cells within viable CD45.2 donor marrow compartment. Each point represents data from one recipient mouse. Horizontal black bars represent means. F) Contribution of lymphoblasts (blasts), granulocytes, or lymphocytes to total marrow, expressed as percentage of total CD45.2 viable cells. Top plot: Gated on viable WBM. Bottom plot: Gated on UHRF1+ WBM. Data expressed as mean values. WT n = 2, wt/wt n = 2, Δ/Δ n = 3. Donor marrow genotypes: WT (*Uhrf1^{wt/wt}*), wt/wt (*Mx1-Cre;Uhrf1^{wt/wt}*), Δ/Δ (*Uhrf1^{Δ/Δ}*).

CHAPTER 4: CONCLUSIONS AND FUTURE DIRECTIONS

In this dissertation, genome-wide gene expression of highly-refined HSPCs from normal and leukemic bone marrow donors was used to develop insights on the molecular mechanisms of normal HSC function and LSC transformation. In studying chronic phase CML LSCs, we were able to identify unique cell surface molecules and mechanistic pathways that may serve as potential CML LSC targets. We were able to isolate highly-enriched leukemic stem cell fractions to avoid contamination by bulk tumor cells and subsequent limitations in defining purely LSC-specific targets. In this way, optimal therapeutic intervention could selectively eliminate the LSC fraction responsible for propagating the tumor, while sparing normal hematopoiesis in the patient. One particularly promising target identified was *DPP4*, or CD26, for which there are FDA-approved inhibitors for the treatment of diabetes mellitus. Although we did not investigate the influence of DPP4 inhibition on patient prognosis, one study reported decreased BCR/ABL1 transcript levels in two patients who were co-treated with a tyrosine kinase and DPP4 inhibitors, demonstrating the successful therapeutic potential of targeting DPP4 in chronic phase CML⁹⁶.

In the second half of our study, we focused on epigenetic regulatory mechanisms in normal hematopoiesis. Understanding the complex mechanisms involved in stem cell function can shed light on critical programs that may be perturbed in leukemic development. We nominated *UHRF1* as an essential epigenetic regulator in normal hematopoiesis and described its role in this process in a murine model. Further investigation could include a look into the mechanism by which UHRF1 regulates stem cell fate decisions in our mouse model, including any alterations in DNA or H3K9 methylation and downstream influence on expression of UHRF1-regulated genes.

Accumulating evidence supports UHRF1 as an oncogene and potential therapeutic target in hematologic malignancies and other cancers. Several UHRF1 knockdown studies have shown reduced cell growth in cervical⁹⁷ and esophageal⁹⁸ squamous cell carcinoma and ovarian⁹⁹, gallbladder¹⁰⁰, breast^{101,102}, and anaplastic thyroid¹⁰³ cancer. Additionally, previous data from our lab showed heterozygous knockout of UHRF1 reduced tumor burden in an APC-driven mouse model of colon cancer. While the data from our hematopoietic model suggests that complete knockout of UHRF1 in a patient would have detrimental, possibly lethal, side-effects in the hematopoietic system, the striking absence of a heterozygous phenotype and the promising results from previous knockdown studies supports the possibility of an optimal therapeutic dose with little harm to normal hematopoiesis. Building on this hypothesis, we could examine the role of UHRF1 in a leukemic model and assess the efficacy of UHRF1 inhibition or depletion on disease progression in mice.

REFERENCES

1. Kondo M, Wagers AJ, Manz MG, et al. Biology of hematopoietic stem cells and progenitors: implications for clinical application. *Annu Rev Immunol*. 2003;21:759-806.
2. Chao MP, Seita J, Weissman IL. Establishment of a normal hematopoietic and leukemia stem cell hierarchy. *Cold Spring Harb Symp Quant Biol*. 2008;73:439-449.
3. Lemischka IR, Raulet DH, Mulligan RC. Developmental potential and dynamic behavior of hematopoietic stem cells. *Cell*. 1986;45(6):917-927.
4. Civin CI, Strauss LC, Brovall C, Fackler MJ, Schwartz JF, Shaper JH. Antigenic analysis of hematopoiesis. III. A hematopoietic progenitor cell surface antigen defined by a monoclonal antibody raised against KG-1a cells. *J Immunol*. 1984;133(1):157-165.
5. Bhatia M, Wang JC, Kapp U, Bonnet D, Dick JE. Purification of primitive human hematopoietic cells capable of repopulating immune-deficient mice. *Proc Natl Acad Sci U S A*. 1997;94(10):5320-5325.
6. Jones RJ, Barber JP, Vala MS, et al. Assessment of aldehyde dehydrogenase in viable cells. *Blood*. 1995;85(10):2742-2746.
7. Fleming HE, Janzen V, Lo Celso C, et al. Wnt signaling in the niche enforces hematopoietic stem cell quiescence and is necessary to preserve self-renewal in vivo. *Cell Stem Cell*. 2008;2(3):274-283.
8. Randall TD, Weissman IL. Phenotypic and functional changes induced at the clonal level in hematopoietic stem cells after 5-fluorouracil treatment. *Blood*. 1997;89(10):3596-3606.
9. Adolfsson J, Borge OJ, Bryder D, et al. Upregulation of Flt3 expression within the bone marrow Lin(-)Sca1(+)c-kit(+) stem cell compartment is accompanied by loss of self-renewal capacity. *Immunity*. 2001;15(4):659-669.
10. Kiel MJ, Radice GL, Morrison SJ. Lack of evidence that hematopoietic stem cells depend on N-cadherin-mediated adhesion to osteoblasts for their maintenance. *Cell Stem Cell*. 2007;1(2):204-217.
11. Goodell MA, Brose K, Paradis G, Conner AS, Mulligan RC. Isolation and functional properties of murine hematopoietic stem cells that are replicating in vivo. *J Exp Med*. 1996;183(4):1797-1806.
12. Harrison DE. Competitive repopulation: a new assay for long-term stem cell functional capacity. *Blood*. 1980;55(1):77-81.
13. Ooi SK, O'Donnell AH, Bestor TH. Mammalian cytosine methylation at a glance. *J Cell Sci*. 2009;122(Pt 16):2787-2791.
14. Doi A, Park IH, Wen B, et al. Differential methylation of tissue- and cancer-specific CpG island shores distinguishes human induced pluripotent stem cells, embryonic stem cells and fibroblasts. *Nat Genet*. 2009;41(12):1350-1353.
15. Ji H, Ehrlich LI, Seita J, et al. Comprehensive methylome map of lineage commitment from haematopoietic progenitors. *Nature*. 2010;467(7313):338-342.
16. Broske AM, Vockentanz L, Kharazi S, et al. DNA methylation protects hematopoietic stem cell multipotency from myeloerythroid restriction. *Nat Genet*. 2009;41(11):1207-1215.
17. Bocker MT, Hellwig I, Breiling A, Eckstein V, Ho AD, Lyko F. Genome-wide promoter DNA methylation dynamics of human hematopoietic progenitor cells during differentiation and aging. *Blood*. 2011;117(19):e182-189.

18. Wilop S, Fernandez AF, Jost E, et al. Array-based DNA methylation profiling in acute myeloid leukaemia. *Br J Haematol*. 2011;155(1):65-72.
19. Figueroa ME, Lugthart S, Li Y, et al. DNA methylation signatures identify biologically distinct subtypes in acute myeloid leukemia. *Cancer Cell*. 2010;17(1):13-27.
20. Vigna E, Recchia AG, Madeo A, et al. Epigenetic regulation in myelodysplastic syndromes: implications for therapy. *Expert Opin Investig Drugs*. 2011;20(4):465-493.
21. Chung YR, Schatoff E, Abdel-Wahab O. Epigenetic alterations in hematopoietic malignancies. *Int J Hematol*. 2012;96(4):413-427.
22. Abdel-Wahab O, Levine RL. Mutations in epigenetic modifiers in the pathogenesis and therapy of acute myeloid leukemia. *Blood*. 2013;121(18):3563-3572.
23. Druker BJ, Talpaz M, Resta DJ, et al. Efficacy and safety of a specific inhibitor of the BCR-ABL tyrosine kinase in chronic myeloid leukemia. *N Engl J Med*. 2001;344(14):1031-1037.
24. Kantarjian H, Talpaz M, O'Brien S, et al. High-dose imatinib mesylate therapy in newly diagnosed Philadelphia chromosome-positive chronic phase chronic myeloid leukemia. *Blood*. 2004;103(8):2873-2878.
25. Cortes J, O'Brien S, Kantarjian H. Discontinuation of imatinib therapy after achieving a molecular response. *Blood*. 2004;104(7):2204-2205.
26. Rousselot P, Huguet F, Rea D, et al. Imatinib mesylate discontinuation in patients with chronic myelogenous leukemia in complete molecular remission for more than 2 years. *Blood*. 2007;109(1):58-60.
27. Graham SM, Jorgensen HG, Allan E, et al. Primitive, quiescent, Philadelphia-positive stem cells from patients with chronic myeloid leukemia are insensitive to STI571 in vitro. *Blood*. 2002;99(1):319-325.
28. Angstreich GR, Matsui W, Huff CA, et al. Effects of imatinib and interferon on primitive chronic myeloid leukaemia progenitors. *Br J Haematol*. 2005;130(3):373-381.
29. Copland M, Hamilton A, Elrick LJ, et al. Dasatinib (BMS-354825) targets an earlier progenitor population than imatinib in primary CML but does not eliminate the quiescent fraction. *Blood*. 2006;107(11):4532-4539.
30. Bhatia R, Holtz M, Niu N, et al. Persistence of malignant hematopoietic progenitors in chronic myelogenous leukemia patients in complete cytogenetic remission following imatinib mesylate treatment. *Blood*. 2003;101(12):4701-4707.
31. Mahon FX, Rea D, Guilhot J, et al. Discontinuation of imatinib in patients with chronic myeloid leukaemia who have maintained complete molecular remission for at least 2 years: the prospective, multicentre Stop Imatinib (STIM) trial. *Lancet Oncol*. 2010;11(11):1029-1035.
32. Hughes TP, Hochhaus A, Branford S, et al. Long-term prognostic significance of early molecular response to imatinib in newly diagnosed chronic myeloid leukemia: an analysis from the International Randomized Study of Interferon and STI571 (IRIS). *Blood*. 2010;116(19):3758-3765.
33. O'Hare T, Zabriskie MS, Eiring AM, Deininger MW. Pushing the limits of targeted therapy in chronic myeloid leukaemia. *Nat Rev Cancer*. 2012;12(8):513-526.
34. Bedi A, Zehnbaauer BA, Collector MI, et al. BCR-ABL gene rearrangement and expression of primitive hematopoietic progenitors in chronic myeloid leukemia. *Blood*. 1993;81(11):2898-2902.

35. Raaijmakers MH, van Emst L, de Witte T, Mensink E, Raymakers RA. Quantitative assessment of gene expression in highly purified hematopoietic cells using real-time reverse transcriptase polymerase chain reaction. *Exp Hematol.* 2002;30(5):481-487.
36. Mahon FX, Belloc F, Lagarde V, et al. MDR1 gene overexpression confers resistance to imatinib mesylate in leukemia cell line models. *Blood.* 2003;101(6):2368-2373.
37. Jiang G, Yang F, Li M, et al. Imatinib (ST1571) provides only limited selectivity for CML cells and treatment might be complicated by silent BCR-ABL genes. *Cancer Biol Ther.* 2003;2(1):103-108.
38. Bonnet D. Normal and leukaemic stem cells. *Br J Haematol.* 2005;130(4):469-479.
39. Christ O, Lucke K, Imren S, et al. Improved purification of hematopoietic stem cells based on their elevated aldehyde dehydrogenase activity. *Haematologica.* 2007;92(9):1165-1172.
40. Gerber JM, Smith BD, Ngwang B, et al. A clinically relevant population of leukemic CD34(+)CD38(-) cells in acute myeloid leukemia. *Blood.* 2012;119(15):3571-3577.
41. Vasiliou V, Pappa A, Estey T. Role of human aldehyde dehydrogenases in endobiotic and xenobiotic metabolism. *Drug Metab Rev.* 2004;36(2):279-299.
42. Gerber JM, Qin L, Kowalski J, et al. Characterization of chronic myeloid leukemia stem cells. *Am J Hematol.* 2011;86(1):31-37.
43. Huang da W, Sherman BT, Lempicki RA. Systematic and integrative analysis of large gene lists using DAVID bioinformatics resources. *Nat Protoc.* 2009;4(1):44-57.
44. Huang da W, Sherman BT, Lempicki RA. Bioinformatics enrichment tools: paths toward the comprehensive functional analysis of large gene lists. *Nucleic Acids Res.* 2009;37(1):1-13.
45. Subramanian A, Tamayo P, Mootha VK, et al. Gene set enrichment analysis: a knowledge-based approach for interpreting genome-wide expression profiles. *Proc Natl Acad Sci U S A.* 2005;102(43):15545-15550.
46. Irizarry RA, Wang C, Zhou Y, Speed TP. Gene set enrichment analysis made simple. *Stat Methods Med Res.* 2009;18(6):565-575.
47. Aryee MJ, Liu W, Engelmann JC, et al. DNA methylation alterations exhibit intraindividual stability and interindividual heterogeneity in prostate cancer metastases. *Sci Transl Med.* 2013;5(169):169ra110.
48. Cicuttini FM, Welch K, Boyd AW. Characterization of CD34+HLA-DR-CD38+ and CD34+HLA-DR-CD38- progenitor cells from human umbilical cord blood. *Growth Factors.* 1994;10(2):127-134.
49. Ashburner M, Ball CA, Blake JA, et al. Gene ontology: tool for the unification of biology. The Gene Ontology Consortium. *Nat Genet.* 2000;25(1):25-29.
50. Kanehisa M, Goto S, Sato Y, Furumichi M, Tanabe M. KEGG for integration and interpretation of large-scale molecular data sets. *Nucleic Acids Res.* 2012;40(Database issue):D109-114.
51. Kanehisa M, Goto S. KEGG: kyoto encyclopedia of genes and genomes. *Nucleic Acids Res.* 2000;28(1):27-30.

52. Shioda T, Kato H, Ohnishi Y, et al. Anti-HIV-1 and chemotactic activities of human stromal cell-derived factor 1alpha (SDF-1alpha) and SDF-1beta are abolished by CD26/dipeptidyl peptidase IV-mediated cleavage. *Proc Natl Acad Sci U S A*. 1998;95(11):6331-6336.
53. Sipkins DA, Wei X, Wu JW, et al. In vivo imaging of specialized bone marrow endothelial microdomains for tumour engraftment. *Nature*. 2005;435(7044):969-973.
54. Deacon CF, Carr RD, Holst JJ. DPP-4 inhibitor therapy: new directions in the treatment of type 2 diabetes. *Front Biosci*. 2008;13:1780-1794.
55. Rose JW. Anti-CD25 immunotherapy: regulating the regulators. *Sci Transl Med*. 2012;4(145):145fs125.
56. Jaras M, Johnels P, Hansen N, et al. Isolation and killing of candidate chronic myeloid leukemia stem cells by antibody targeting of IL-1 receptor accessory protein. *Proc Natl Acad Sci U S A*. 2010;107(37):16280-16285.
57. Barreyro L, Will B, Bartholdy B, et al. Overexpression of IL-1 receptor accessory protein in stem and progenitor cells and outcome correlation in AML and MDS. *Blood*. 2012;120(6):1290-1298.
58. Dinarello CA, Simon A, van der Meer JW. Treating inflammation by blocking interleukin-1 in a broad spectrum of diseases. *Nat Rev Drug Discov*. 2012;11(8):633-652.
59. Ren R. Mechanisms of BCR-ABL in the pathogenesis of chronic myelogenous leukaemia. *Nat Rev Cancer*. 2005;5(3):172-183.
60. Biernacki MA, Marina O, Zhang W, et al. Efficacious immune therapy in chronic myelogenous leukemia (CML) recognizes antigens that are expressed on CML progenitor cells. *Cancer Res*. 2010;70(3):906-915.
61. Bruns I, Czibere A, Fischer JC, et al. The hematopoietic stem cell in chronic phase CML is characterized by a transcriptional profile resembling normal myeloid progenitor cells and reflecting loss of quiescence. *Leukemia*. 2009;23(5):892-899.
62. Flis K, Irvine D, Copland M, Bhatia R, Skorski T. Chronic myeloid leukemia stem cells display alterations in expression of genes involved in oxidative phosphorylation. *Leuk Lymphoma*. 2012;53(12):2474-2478.
63. Pienta KJ, Machiels JP, Schrijvers D, et al. Phase 2 study of carlumab (CNTO 888), a human monoclonal antibody against CC-chemokine ligand 2 (CCL2), in metastatic castration-resistant prostate cancer. *Invest New Drugs*. 2012.
64. Schwartz GK, LoRusso PM, Dickson MA, et al. Phase I study of PD 0332991, a cyclin-dependent kinase inhibitor, administered in 3-week cycles (Schedule 2/1). *Br J Cancer*. 2011;104(12):1862-1868.
65. Flaherty KT, Lorusso PM, Demichele A, et al. Phase I, dose-escalation trial of the oral cyclin-dependent kinase 4/6 inhibitor PD 0332991, administered using a 21-day schedule in patients with advanced cancer. *Clin Cancer Res*. 2012;18(2):568-576.
66. Monteleone G, Fantini MC, Onali S, et al. Phase I clinical trial of Smad7 knockdown using antisense oligonucleotide in patients with active Crohn's disease. *Mol Ther*. 2012;20(4):870-876.
67. Zhu X, Wang L, Zhang B, Li J, Dou X, Zhao RC. TGF-beta1-induced PI3K/Akt/NF-kappaB/MMP9 signalling pathway is activated in Philadelphia chromosome-positive chronic myeloid leukaemia hemangioblasts. *J Biochem*. 2011;149(4):405-414.

68. Naka K, Hoshii T, Muraguchi T, et al. TGF-beta-FOXO signalling maintains leukaemia-initiating cells in chronic myeloid leukaemia. *Nature*. 2010;463(7281):676-680.
69. Moller GM, Frost V, Melo JV, Chantry A. Upregulation of the TGFbeta signalling pathway by Bcr-Abl: implications for haemopoietic cell growth and chronic myeloid leukaemia. *FEBS Lett*. 2007;581(7):1329-1334.
70. Roberts AB, Wakefield LM. The two faces of transforming growth factor beta in carcinogenesis. *Proc Natl Acad Sci U S A*. 2003;100(15):8621-8623.
71. Bierie B, Moses HL. Tumour microenvironment: TGFbeta: the molecular Jekyll and Hyde of cancer. *Nat Rev Cancer*. 2006;6(7):506-520.
72. Storey JD. A direct approach to false discovery rates. *J R Statist Soc B*. 2002;64(Part 3):479-498.
73. Figueroa ME, Abdel-Wahab O, Lu C, et al. Leukemic IDH1 and IDH2 mutations result in a hypermethylation phenotype, disrupt TET2 function, and impair hematopoietic differentiation. *Cancer Cell*. 2010;18(6):553-567.
74. Ley TJ, Ding L, Walter MJ, et al. DNMT3A mutations in acute myeloid leukemia. *N Engl J Med*. 2010;363(25):2424-2433.
75. Helin K, Dhanak D. Chromatin proteins and modifications as drug targets. *Nature*. 2013;502(7472):480-488.
76. Trowbridge JJ, Snow JW, Kim J, Orkin SH. DNA methyltransferase 1 is essential for and uniquely regulates hematopoietic stem and progenitor cells. *Cell Stem Cell*. 2009;5(4):442-449.
77. Bostick M, Kim JK, Esteve PO, Clark A, Pradhan S, Jacobsen SE. UHRF1 plays a role in maintaining DNA methylation in mammalian cells. *Science*. 2007;317(5845):1760-1764.
78. Sharif J, Muto M, Takebayashi S, et al. The SRA protein Np95 mediates epigenetic inheritance by recruiting Dnmt1 to methylated DNA. *Nature*. 2007;450(7171):908-912.
79. Unoki M, Nishidate T, Nakamura Y. ICBP90, an E2F-1 target, recruits HDAC1 and binds to methyl-CpG through its SRA domain. *Oncogene*. 2004;23(46):7601-7610.
80. Karagianni P, Amazit L, Qin J, Wong J. ICBP90, a novel methyl K9 H3 binding protein linking protein ubiquitination with heterochromatin formation. *Mol Cell Biol*. 2008;28(2):705-717.
81. Citterio E, Papait R, Nicassio F, et al. Np95 is a histone-binding protein endowed with ubiquitin ligase activity. *Mol Cell Biol*. 2004;24(6):2526-2535.
82. Fang J, Cheng J, Wang J, et al. Hemi-methylated DNA opens a closed conformation of UHRF1 to facilitate its histone recognition. *Nat Commun*. 2016;7:11197.
83. Haferlach T, Kohlmann A, Wicczorek L, et al. Clinical utility of microarray-based gene expression profiling in the diagnosis and subclassification of leukemia: report from the International Microarray Innovations in Leukemia Study Group. *J Clin Oncol*. 2010;28(15):2529-2537.
84. Guan D, Factor D, Liu Y, Wang Z, Kao HY. The epigenetic regulator UHRF1 promotes ubiquitination-mediated degradation of the tumor-suppressor protein promyelocytic leukemia protein. *Oncogene*. 2013;32(33):3819-3828.

85. Bronner C, Achour M, Arima Y, Chataigneau T, Saya H, Schini-Kerth VB. The UHRF family: oncogenes that are drugable targets for cancer therapy in the near future? *Pharmacol Ther.* 2007;115(3):419-434.
86. Gerber JM, Gucwa JL, Esopi D, et al. Genome-wide comparison of the transcriptomes of highly enriched normal and chronic myeloid leukemia stem and progenitor cell populations. *Oncotarget.* 2013;4(5):715-728.
87. Medvedeva YA, Lennartsson A, Ehsani R, et al. EpiFactors: a comprehensive database of human epigenetic factors and complexes. *Database (Oxford).* 2015;2015:bav067.
88. Lo Celso C, Scadden D. Isolation and transplantation of hematopoietic stem cells (HSCs). *J Vis Exp.* 2007(2):157.
89. Nishio N, Hisha H, Ogata H, et al. Changes in markers, receptors and adhesion molecules expressed on murine hemopoietic stem cells after a single injection of 5-fluorouracil. *Stem Cells.* 1996;14(5):584-591.
90. Dolence JJ, Gwin K, Frank E, Medina KL. Threshold levels of Flt3-ligand are required for the generation and survival of lymphoid progenitors and B-cell precursors. *Eur J Immunol.* 2011;41(2):324-334.
91. Herrera-Merchan A, Arranz L, Ligos JM, de Molina A, Dominguez O, Gonzalez S. Ectopic expression of the histone methyltransferase Ezh2 in haematopoietic stem cells causes myeloproliferative disease. *Nat Commun.* 2012;3:623.
92. Moran-Crusio K, Reavie L, Shih A, et al. Tet2 loss leads to increased hematopoietic stem cell self-renewal and myeloid transformation. *Cancer Cell.* 2011;20(1):11-24.
93. Morin RD, Johnson NA, Severson TM, et al. Somatic mutations altering EZH2 (Tyr641) in follicular and diffuse large B-cell lymphomas of germinal-center origin. *Nat Genet.* 2010;42(2):181-185.
94. Waskow C, Paul S, Haller C, Gassmann M, Rodewald HR. Viable c-Kit(W/W) mutants reveal pivotal role for c-kit in the maintenance of lymphopoiesis. *Immunity.* 2002;17(3):277-288.
95. Kumar R, Fossati V, Israel M, Snoeck HW. Lin-Sca1+kit- bone marrow cells contain early lymphoid-committed precursors that are distinct from common lymphoid progenitors. *J Immunol.* 2008;181(11):7507-7513.
96. Herrmann H, Sadovnik I, Cerny-Reiterer S, et al. Dipeptidylpeptidase IV (CD26) defines leukemic stem cells (LSC) in chronic myeloid leukemia. *Blood.* 2014;123(25):3951-3962.
97. Ge TT, Yang M, Chen Z, Lou G, Gu T. UHRF1 gene silencing inhibits cell proliferation and promotes cell apoptosis in human cervical squamous cell carcinoma CaSki cells. *J Ovarian Res.* 2016;9(1):42.
98. Yang C, Wang Y, Zhang F, et al. Inhibiting UHRF1 expression enhances radiosensitivity in human esophageal squamous cell carcinoma. *Mol Biol Rep.* 2013;40(9):5225-5235.
99. Yan F, Shao LJ, Hu XY. Knockdown of UHRF1 by lentivirus-mediated shRNA inhibits ovarian cancer cell growth. *Asian Pac J Cancer Prev.* 2015;16(4):1343-1348.
100. Qin Y, Wang J, Gong W, et al. UHRF1 depletion suppresses growth of gallbladder cancer cells through induction of apoptosis and cell cycle arrest. *Oncol Rep.* 2014;31(6):2635-2643.

101. Fang L, Shanqu L, Ping G, et al. Gene therapy with RNAi targeting UHRF1 driven by tumor-specific promoter inhibits tumor growth and enhances the sensitivity of chemotherapeutic drug in breast cancer in vitro and in vivo. *Cancer Chemother Pharmacol.* 2012;69(4):1079-1087.
102. Yan F, Tan XY, Geng Y, Ju HX, Gao YF, Zhu MC. Inhibition effect of siRNA-downregulated UHRF1 on breast cancer growth. *Cancer Biother Radiopharm.* 2011;26(2):183-189.
103. Wang BC, Lin GH, Wang B, et al. UHRF1 suppression promotes cell differentiation and reduces inflammatory reaction in anaplastic thyroid cancer. *Oncotarget.* 2016.

CURRICULUM VITAE

Jessica L. Gucwa

Contact Information

Address: 1806 Thames Street
Apt 23
Baltimore, MD 21231

Tel: (716) 481-0095

Email: jessica.gucwa@gmail.com

Personal Data

Date of Birth: April 22, 1985

Place of Birth: Buffalo, NY

Education

2016 Ph.D., Cellular and Molecular Medicine, Johns Hopkins University, Baltimore, MD

2007 B.S., Biochemistry, SUNY Geneseo, Geneseo, NY. Summa Cum Laude.

Research Experience

2007-Present Graduate student, Cellular and Molecular Medicine Program, Johns Hopkins University School of Medicine, Baltimore, MD
Thesis Advisors: William Nelson, M.D., Ph.D., Srinivasan Yegnasubramanian, M.D., Ph.D
Thesis: Transcriptional and Epigenetic Regulatory Programs in Hematopoiesis and Leukemogenesis

2006-2007 Undergraduate Research Assistant, SUNY Geneseo, Geneseo NY
Principal Investigator: Wendy Pogozielski, Ph.D.
Project: Real-time PCR Quantification of the 5-kb Common Deletion in Human Mitochondrial DNA Induced by Gamma Radiation

June-August 2006 National Science Foundation Fellowship, Roswell Park Cancer Institute Summer Research Program, Roswell Park Cancer Institute, Buffalo NY
Principal Investigator: Elizabeth Repasky, Ph.D.
Project: The Role of NFkB in the Resistance of Leukemia Cells to Apo2L/TRAIL

- June-August 2005 Immunology Research Assistant, Roswell Park Cancer Institute, Buffalo NY
Principal Investigator: Elizabeth Repasky, Ph.D.
Project: Targeting the Epidermal Growth Factor Receptor with Tarceva for the Potential Treatment of Pancreatic Cancer
- June-August 2004 Immunology Research Volunteer, Roswell Park Cancer Institute, Buffalo NY
Principal Investigator: Elizabeth Repasky, Ph.D.

Teaching Experience

- 2009 Pollard Scholar, graduate student tutor for Pathways and Regulation course
- 2008 Pollard Scholar, graduate student tutor for Molecular Biology course
- 2005-2007 General Chemistry, laboratory instructor

Publications

Ghiaur G, Yegnasubramanian S, Perkins B, **Gucwa JL**, Gerber JM, Jones RJ. Regulation of human hematopoietic stem cell self-renewal by the microenvironment's control of retinoic acid signaling. Proc Natl Acad Sci U S A. 2013 Oct 1;110(40):16121-6.

Gerber JM*, **Gucwa JL***, Esopi D, Gurel M, Haffner MC, Vala M, Nelson WG, Jones RJ, Yegnasubramanian S. Genome-wide comparison of the transcriptomes of highly enriched normal and chronic myeloid leukemia stem and progenitor cell populations. Oncotarget. 2013 May;4(5):715-28. *Authors contributed equally to this work.

Gucwa JL, Vaghasia A, Walker D, Esopi D, Singer B, Haffner MC, Castagna N, Nelson WG, Ghiaur G, Yegnasubramanian S. The epigenetic regulator UHRF1 in a murine model of normal adult hematopoiesis. Manuscript in prep.

Presentations

Identification of putative CML stem cell therapeutic targets, poster, Cellular and Molecular Medicine retreat, 2011.

Investigating the role of reactive oxygen species in the poor prognosis of AML patients with FLT3/ITD mutations, poster, Cellular and Molecular Medicine retreat, 2009.

Investigating hypermethylation in cancer by MeDIP, talk, CMM Rotation Presentation, 2008.

Understanding residual viremia in HIV-1 infected patients with undetectable viral loads, poster, CMM Rotation Presentation, 2007.

A Radiation Dose-Dependent Increase in the 4977-bp Common Deletion in Mitochondrial DNA in Respiration-Deficient Pearson's Syndrome Lymphoblasts, poster, FASEB Experimental Biology Conference, Washington, DC, 2007.

A Radiation Dose-Dependent Increase in the 4977-bp Common Deletion in Mitochondrial DNA in Respiration-Deficient Pearson's Syndrome Lymphoblasts, poster, SUNY Geneseo Undergraduate Research Conference, Geneseo, NY, 2007.

The Role of NFkB in the Resistance of Leukemia Cells to Apo2L/TRAIL, poster and talk, Roswell Park Cancer Institute National Science Foundation Fellow Annual Research Symposium, Buffalo, NY, 2006.

Induction of a Mitochondrial DNA Deletion by Gamma Radiation, poster, SUNY Geneseo Undergraduate Research Conference, Geneseo, NY, 2006.

Induction of a Mitochondrial DNA Deletion by Gamma Radiation, poster, American Chemical Society Undergraduate Research Symposium, Brockport, NY, 2006.

Undergraduate Awards and Honors

Jackson-Ulmer Biochemistry Award 2007

SUNY Chancellor's Award for Student Excellence 2007

Myrtle Merritt Scholar Athlete Award 2007

SUNYAC Commissioner's Academic List 2005-2007

SUNYAC All-Academic Team 2004-2007

Barry M. Goldwater Scholarship 2006

Undergraduate Award for Achievement in Organic Chemistry 2004-2005

Geneseo Alumni Fellows Scholarship 2004

Undergraduate Honor Societies

Phi Eta Sigma National Honor Society member

Golden Key International Honour Society member

Beta Phi Beta Kappa Society-Alpha Delta Chapter

Gamma Sigma Epsilon Chemistry Honor Society

Beta Beta Biological Honor Society-Lambda Kappa Chapter